TECHNICAL REPORT STANDARD TITLE PAGE

1. Report No.	2. Government Accession No.	3. Recipient's Catalog No.
TX-92-1923-1		

4. Title and Subtitle	5. Report Date
Influence of Asphalt Layering and Surface Treatments on Asphalt and Base Layer Thickness Computations Using Radar	September 1992
	6. Performing Organization Code

7. Author(s)	8. Performing Organization Report No.
Ken Maser (Infrasense, Cambridge, MA) Tom Scullion (Texas Transportation Institute)	Research Report 1923-1

9. Performing Organization Name and Address	10. Work Unit No.
Texas Transportation Institute Highway Materials Division Texas A&M University College Station, TX 77843-3135	11. Contract or Grant No. Study No. 2-18-91-1923-1

12. Sponsoring Agency Name and Address	13. Type of Report and Period Covered
Texas Department of Transportation Planning Division P.O. Box 5051 Austin, TX 78763	Final
	14. Sponsoring Agency Code

15. Supplementary Notes

Research performed for the State of Texas.
Research Study Title " Influence of Asphalt Layering and Surface Treatments on Asphalt and Base Layer Thickness Computations Using Radar

16. Abstract

This study has been carried out with the specific objective of evaluating the influence of thin overlays and surface treatments on the accuracy of pavement thickness calculations using radar. Nine SHRP GPS and SPS sites located on three Texas primary roads were surveyed with radar: two each with a slurry seal, a chip seal, a new overlay, and an old overlay, and one of original construction. Cores were taken at accessible locations to obtain ground truth for asphalt and base thickness.

The radar and core data was analyzed to determine the influence of the overlays on the accuracy of the radar computations, and to evaluate analytical techniques which would lead to the highest degree of accuracy. The results show that the thickness of overlays as thin as 1" can be accurately evaluated. The results also show that the overall accuracy of asphalt and base thickness calculations can be improved if the appropriate analytical techniques are applied. In certain circumstances, however (one thin low density overlay and one chip seal), the accuracy was reduced. The accuracy of the base thickness computations were improved (+/- 9.5%) from what was determined in previous studies on these same sites. This improvement was achieved by considering the thin overlays in the radar model, and by implementing a threshold algorithm for acceptance of base thickness data.

Further evidence was generated to support the capability of radar to detect moisture within the asphalt layers. Future studies should seek to confirm this evidence with controlled field sampling and laboratory moisture tests.

17. Key Words	18. Distribution Statement
Ground Penetrating Radar, Thickness Determination, Pavements, Maintenance Field Testing, NDT, Research	No Restrictions. This document is available to the public through the National Information Service 5285 Port Royal Road Springfield, VA 22161

19. Security Classif. (of this report)	20. Security Classif. (of this page)	21. No. of Pages	22. Price
Unclassified	Unclassified	89	

Form DOT F 1700.7 (8-69)

INFLUENCE OF ASPHALT LAYERING AND SURFACE TREATMENTS ON ASPHALT AND BASE LAYER THICKNESS COMPUTATIONS USING RADAR

by Kenneth R. Maser
INFRASENSE, Inc.

and

Tom Scullion
Texas Transportation Institute

TTI Report 1923-1
Final Report

Research Conducted for

Texas Department of Transportation

by

Texas Transportation Institute
Texas A&M University

September 1992

METRIC (SI*) CONVERSION FACTORS

APPROXIMATE CONVERSIONS TO SI UNITS

Symbol	When You Know	Multiply By	To Find	Symbol
LENGTH				
in	inches	2.54	centimetres	cm
ft	feet	0.3048	metres	m
yd	yards	0.914	metres	m
mi	miles	1.61	kilometres	km
AREA				
in^2	square inches	645.2	centimetres squared	cm^2
ft^2	square feet	0.0929	metres squared	m^2
yd^2	square yards	0.836	metres squared	m^2
mi^2	square miles	2.59	kilometres squared	km^2
ac	acres	0.395	hectares	ha
MASS (weight)				
oz	ounces	28.35	grams	g
lb	pounds	0.454	kilograms	kg
T	short tons (2000 lb)	0.907	megagrams	Mg
VOLUME				
fl oz	fluid ounces	29.57	millilitres	mL
gal	gallons	3.785	litres	L
ft^3	cubic feet	0.0328	metres cubed	m^3
yd^3	cubic yards	0.0765	metres cubed	m^3

NOTE: Volumes greater than 1000 L shall be shown in m^3.

TEMPERATURE (exact)

°F	Fahrenheit temperature	5/9 (after subtracting 32)	Celsius temperature	°C

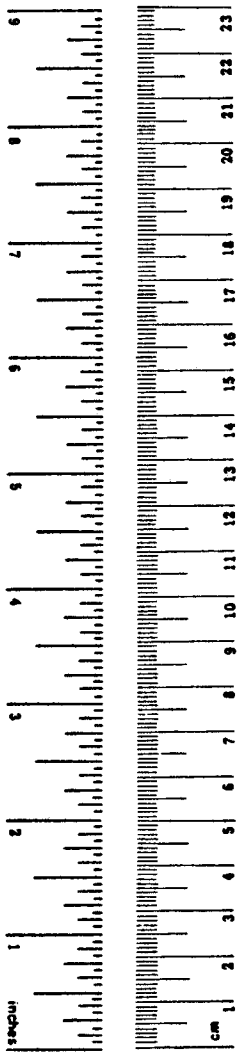

APPROXIMATE CONVERSIONS TO SI UNITS

Symbol	When You Know	Multiply By	To Find	Symbol
LENGTH				
mm	millimetres	0.039	inches	in
m	metres	3.28	feet	ft
m	metres	1.09	yards	yd
km	kilometres	0.621	miles	mi
AREA				
mm^2	millimetres squared	0.0016	square inches	in^2
m^2	metres squared	10.764	square feet	ft^2
km^2	kilometres squared	0.39	square miles	mi^2
ha	hectores (10 000 m^2)	2.53	acres	ac
MASS (weight)				
g	grams	0.0353	ounces	oz
kg	kilograms	2.205	pounds	lb
Mg	megagrams (1 000 kg)	1.103	short tons	T
VOLUME				
mL	millilitres	0.034	fluid ounces	fl oz
L	litres	0.264	gallons	gal
m^3	metres cubed	35.315	cubic feet	ft^3
m^3	metres cubed	1.308	cubic yards	yd^3

TEMPERATURE (exact)

°C	Celsius temperature	9/5 (then add 32)	Fahrenheit temperature	°F

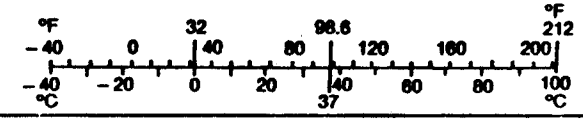

These factors conform to the requirement of FHWA Order 5190.1A.

* SI is the symbol for the International System of Measurements

ABSTRACT

Recent studies of using Ground Penetrating Radar to determine pavement thickness yielded accuracies of +/- 5% to 7.5% for asphalt thickness and +/- 12% for base thickness. The results have stimulated additional interest regarding the influence of surface treatments and thin overlays on radar thickness computations. This study has been carried out with the specific objective of evaluating the influence of thin overlays and surface treatments on the accuracy of pavement thickness calculations using radar. Nine SHRP GPS and SPS sites located on three Texas primary roads were surveyed with radar: two each with a slurry seal, a chip seal, a new overlay, and an old overlay, and one of original construction. Cores were taken at accessible locations to obtain ground truth for asphalt and base thickness.

The radar and core data was analyzed to determine the influence of the overlays on the accuracy of the radar computations, and to evaluate analytical techniques which would lead to the highest degree of accuracy. The results show that the thickness of overlays as thin as 1" can be accurately evaluated. The results also show that the overall accuracy of asphalt and base thickness calculations can be improved if the appropriate analytical techniques are applied. In certain circumstances, however (one thin low density overlay and one chip seal), the accuracy was reduced. The accuracy of the base thickness computations were improved (+/- 9.5%) from what was determined in previous studies on these same sites. This improvement was achieved by considering the thin overlays in the radar model, and by implementing a threshold algorithm for acceptance of base thickness data.

Further evidence was generated to support the capability of radar to detect moisture within the asphalt layers. Future studies should seek to confirm this evidence with controlled field sampling and laboratory moisture tests.

Comparison studies carried out on data obtained from radar systems used in the previous and current research revealed small differences in their performance characteristics. The system used in the previous work (PULSE Radar RODAR II) appears to produce better resolution of base thickness, while the system used in the current work (Penetradar PS-24) produced more accurate thickness values for the surface layers.

DISCLAIMER

The contents of this report reflect the views of the author (s) who is (are) responsible for the facts and the accuracy of the data presented herein.

This report is not intended to constitute a standard, specifications or regulation and does not necessarily represent the views or policy of the FHWA or Texas Department of Transportation. Additionally, this report is not intended for construction, bidding, or permit purposes.

IMPLEMENTATION STATEMENT

The work presented in this report gives further evidence that there are several major applications of Ground Penetration Radar Technology that are ready for implementation. GPR can be used to measure layer thicknesses of flexible pavements, and results in other studies indicate that it can be used to detect pavement defects, such as stripping and moisture related problems beneath slabs.

ACKNOWLEDGEMENT

The authors would like to acknowledge Texas Department of Transportation for their support of this work. Rob Harris, P.E. and Bob Briggs, P.E. were the Texas DOT representatives who initiated the study. The staff of District 11 and 17 are acknowledged for their assistance with ground truth testing and traffic control.

TABLE OF CONTENTS

Abstract iii
Disclaimer iv
Implementation Statement v
Acknowledgement vi
Table of Contents vii
List of Figures ix
1. Background 1
2. Research Approach 3
3. Description of the Test Sites 5
4. Radar Data Collection 11
   4.1 Equipment & Data Characterization 11
   4.2 Calibration Tests 11
   4.3 Survey Procedures 13
5. Radar Data Analysis 15
   5.1 Data Analysis Principles & Software 15
   5.2 Project Specific Software Modifications 16
   5.3 Example of Layer Thickness Calculation 16
6. Ground Truth 20
7. Results 21
   7.1 Comparison of Repeat Surveys 21
      7.1.1 Comparisons for SH30 21
      7.1.2 Comparisons for SH105 27
   7.2 Evaluation of Thin Overlays 32
      7.2.1 Thin Overlay on SH30 32
      7.2.2 Thin Overlay on SH105 33
      7.2.3 US190 Low Density Overlay 45
   7.3 Slurry and Chip Seals 50
      7.3.1 Slurry Seal on SH30 53
      7.3.2 Chip Seal on SH30 56
      7.3.3 Slurry Seal on SH105 60
      7.3.4 Chip Seal on SH105 64
   7.4 Correlations between Radar and Cores 68
8. Discussion 72
   8.1 Comparison of Penetradar PS-24 and
      Pulse Radar R-II Equipment 72

TABLE OF CONTENTS (CON'T)

8.2 Thin Overlays 72
8.3 Slurry and Chip Seals 73
8.4 Moisture in the Asphalt Layers 73
9. Conclusions 75
References 76
Appendix: Summary of Radar vs. Cores 79

LIST OF FIGURES

Figure 1 - Pavement Sections Tested in this Study 6
Figure 2 - Photograph Showing Thin Overlay on SH30 9
Figure 3 - Photograph Showing Chip Seal 9
Figure 4 - Photograph Showing Slurry Seal 10
Figure 5 - Photograph of Penetradar Equipment on Van 12
Figure 6 - Photograph of Equipment in Van 12
Figure 7 - Photograph of Lab Height Calibration Test 18
Figure 8 - Typical GPR Traces from a Control Box Containing Six Inches of Asphalt Over a Six Inch Granular Base. The "WINDOWS" are User Specified to Permit Peak Detection and Layer Thickness Calculation 19
Figure 9 - SH 30 GPS Asphalt Thickness 23
Figure 10 - SH 30 GPS Base Thickness 24
Figure 11 - SH 30 GPS Asphalt Dielectric Constant 25
Figure 12 - SH 30 GPS Normalized Base/Subgrade Reflection 26
Figure 13 - SH 105 GPS Asphalt Thickness 28
Figure 14 - SH 105 GPS Asphalt Dielectric Constant 29
Figure 15 - SH 105 GPS Base Thickness 30
Figure 16 - SH 105 GPS Normalized Base/Subgrade Reflection 31
Figure 17 - Raw Waveforms at the Beginning of SH30 Thin Overlay . . 34
Figure 18 - Waveforms at the Beginning of SH30 Thin Overlay Processed by Removing the Surface Reflection 35
Figure 19 - SH30: Thickness of Overlay and Dielectric Constant of Original Pavement 36
Figure 20 - SH30 Total Asphalt Thickness in Overlay Section 37
Figure 21 - Raw Waveforms at the Beginning of SH105 Thin Overlay . 39
Figure 22 - Waveforms at the Beginning of SH105 Thin Overlay Processed by Removing the Surface Reflection 40
Figure 23 - SH105 Total Asphalt Thickness in the Overlay Section 41
Figure 24 - SH105 Asphalt Dielectric Constant in the Overlay Section 42

LIST OF FIGURES (CON'T)

Figure 25 - SH105 Base Dielectric Constant in the Overlay Section 43
Figure 26 - SH105 Base Thickness in the Overlay Section 44
Figure 27 - Surface Dielectric Constant on US 190 47
Figure 28 - Asphalt Thickness in US 190 48
Figure 29 - US 190: Correlation of Surface Dielectric with Transverse Cracks 49
Figure 30 - SH30 Waveforms Showing Effect of Slurry Seal 51
Figure 31 - SH30 Asphalt Thickness in the Slurry Seal Section . . . 52
Figure 32 - SH30 Base Thickness in the Slurry Seal Section 54
Figure 33 - SH30 Normalized Base/Subgrade Reflection in Slurry Seal Section 55
Figure 34 - SH30 Asphalt Thickness in the Chip Seal Section 57
Figure 35 - SH30 Base Thickness in the Chip Seal Section 58
Figure 36 - SH30 Normalized Base/Subgrade Reflection in Chip Seal Section 59
Figure 37 - SH105 Asphalt Thickness in the Slurry Seal Section . . 61
Figure 38 - SH105 Base Thickness in the Slurry Seal Section 62
Figure 39 - SH105 Normalized Base/Subgrade Reflection in Slurry Seal Section 63
Figure 40 - SH105 Asphalt Thickness in the Chip Seal Section . . . 65
Figure 41 - SH105 Base Thickness in the Chip Seal Section 66
Figure 42 - SH105 Normalized Base/Subgrade Reflection in Chip Seal Section 67
Figure 43 - Cores vs. Radar for Asphalt Thickness 70
Figure 44 - Cores vs. Radar for Base Thickness 71
Figure 45 - Metal Plate Reflection using the PS-24 Antenna 74

CHAPTER 1
BACKGROUND

Recent evaluations of Ground Penetrating Radar (GPR) for the computation of pavement layer thickness have produced favorable results. These results have been based on the use of air-coupled horn antennas, and on the use of software which applies wave propagation models to the raw radar waveforms. The results of a 1990 Texas project (Maser, 1990; Maser and Scullion, 1991), a Kansas project (Maser, 1991; Roddis, et. al., 1992) and a Phase I Florida project (Fernando and Maser, 1992), show accuracies of 5% to 7.5% on asphalt thickness, and 9% to 12% for base thickness. These studies have covered 20 diverse pavement sections, and the results are based on correlations with data from over 200 cores.

Certain questions were raised in these initial studies which are of interest in future applications. For example, it was noticed that the presence of layering within the asphalt creates reflections in the radar data which have to be taken into account in order to obtain accurate thickness results. Also, interest has been expressed in obtaining greater accuracy in the computation of the base layer thickness.

The overall objective of the work described in this report is to (a) evaluate conditions which affect the accuracy of radar-based pavement layer thickness calculations; and (b) develop approaches which deal with these conditions in a manner which maximizes the accuracy. The specific conditions of interest are the presence of thin overlays and surface treatments. In the context of this evaluation, it is also of interest to assess the capability of radar to accurately measure overlay thickness.

A secondary objective of the work has been to assess the differences between radar systems and the capabilities and limitations of different data analysis techniques. The surveys carried out under the 1990 Texas project utilized a *Pulse Radar R-II radar system along with their RDAS data acquisition system. The surveys carried out under this (current) project have used TTI's *Penetradar radar system, coupled with TTI's internally developed data acquisition system. The data analysis for this

* Mention of commercial hardware or software throughout this report does not constitute an endorsement by the Texas Transportation Institute or the Texas Department of Transportation.

project has been carried out using INFRASENSE's current *PAVLAYER software, which has been substantially developed since the initial Texas project.

CHAPTER 2
RESEARCH APPROACH

In the initial GPR Study in Texas (Maser and Scullion, 1991) data was collected and processed on several General Pavement Sections of the Strategic Highway Research Program (SHRP). Two of these sites were subsequently incorporated into the Special Pavement Studies on Maintenance Effectiveness. Each of these sites had 4 maintenance treatments applied. In the earlier work the sections were tested before placement of the SPS Maintenance treatments. The approach in this follow up survey provided the following: (a) the ability to conduct repeat surveys on previously surveyed sites using the new Penetradar System and TTI software; and (b) the ability to focus on the influence of thin overlays, chip seals, and slurry seals under conditions where the pre-existing pavement has been extensively evaluated.

The SPS sites are adjacent to the GPS sites, and most have a 100 foot transition section where the surface treatment has been applied on either end of the 500 foot test site. These transition sections afforded the opportunity to collect verification cores without disturbance to the SPS site. Also, the untreated sections between the SPS sections afforded the research team the opportunity to look at data with and without surface treatment. These comparisons highlighted the influence of the surface treatment in the radar data. An additional GPS site containing thin asphalt layers of varying properties has also been included to provide further data on the influence of layering.

The radar data has been analyzed using PAVLAYER to compute layer thicknesses, and thickness predictions are compared to core samples. For the original GPS sites, the following analyses have been carried out: (1) a recalculation of layer thickness using the 1990 Pulse Radar data with the current PAVLAYER software; (2) a calculation of the pavement layer thicknesses using the data collected in 1991 with the Penetradar/TTI system. These analyses have been used to evaluate the differences in the performance characteristics of the two radar systems.

For SPS sections and the new GPS section, two different analyses are carried out - one in which the surface treatment is ignored, and one in

which an attempt is made to model the surface treatment as a separate layer. The results of these analyses have been compared to cores to determine which represents the better model.

CHAPTER 3
DESCRIPTION OF TEST SITES

Data for this project was collected on the following test sites on State Highway 30 near Huntsville, State Highway 105 near Navasota, and on US Highway 190 near Livingston. Figure 1 shows the nominal pavement cross sections at each of these sites. Below is a description of the surveys conducted at each site.

1) State Highway 30 GPS and SPS Sections

Surveyed in the right wheelpath and in the center of the lane, in two survey runs:

Run 1
- Begins 500 feet before GPS section
- 0-500 transition (surveyed in 1990)
- 500-1000 GPS section (surveyed in 1990)
- 1000-1500 transition (surveyed in 1990)

- 1500-2000 SPS thin overlay
- 2000-2198 transition

- 2198-2918 SPS slurry seal
- 2918-2996 transition
- 2996 end

Run 2 - Right wheelpath
- Begins 400 feet before chip seal

- 0-400 transition
- 400-500 chip seal
- 500-1000 SPS chip seal
- 1000-1100 chip seal
- 1100-1500 transition
- 1500 end

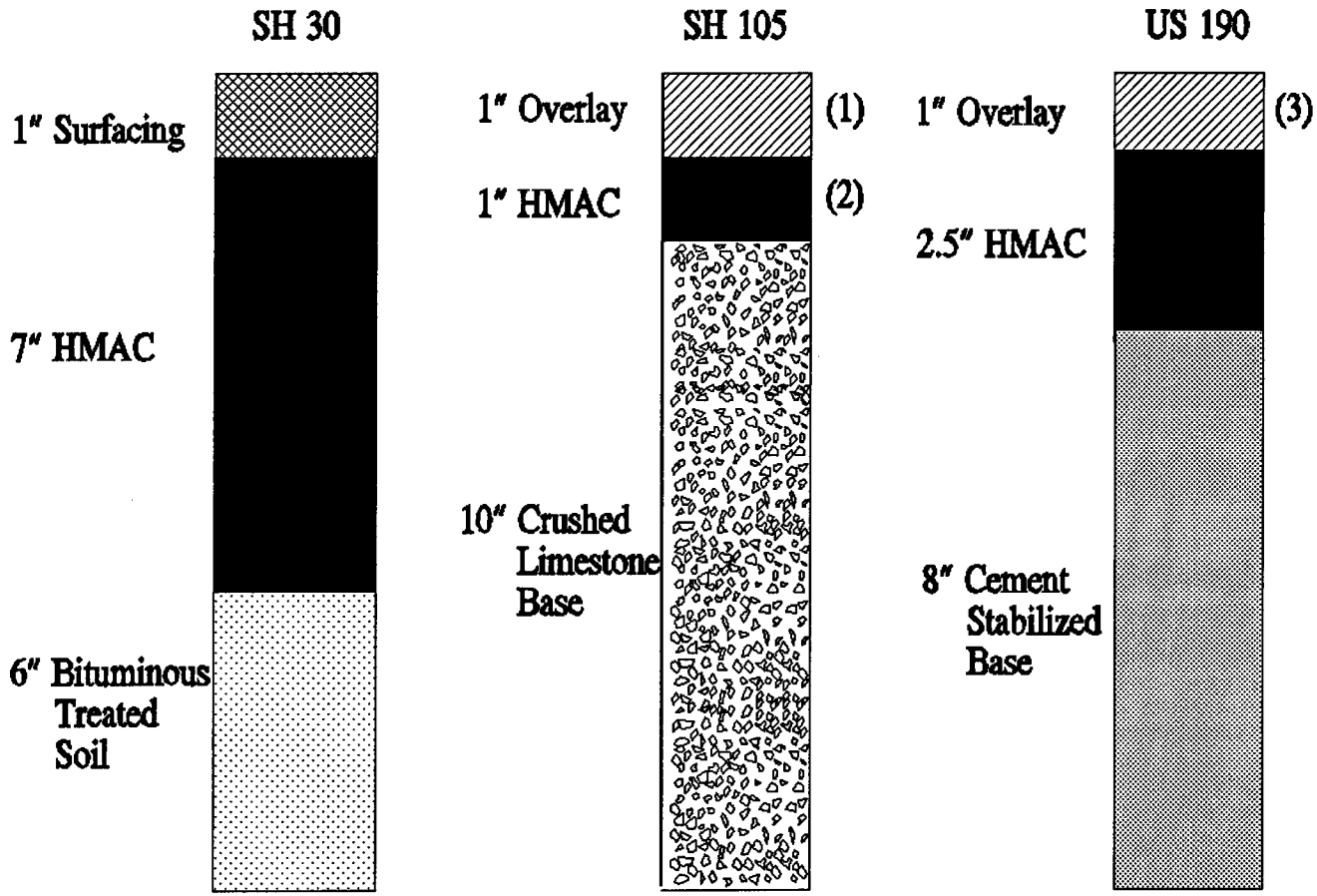

(1) 50% Limestone, 50% Iron Ore Aggregated
(2) 100% Limestone Aggregate
(3) Lightweight Expanded Aggregate

Figure 1. Pavement Sections Tested in this Study.

2) State Highway 105, GPS and SPS Sections

Surveyed in the right wheelpath

Begins 100 ft. before thin overlay
0-100 transition
100-200 thin overlay
200-700 SPS 48H310, thin overlay
700-800 thin overlay

800-1100 transition
1100-1200 slurry seal
1200-1700 SPS slurry seal
1700-1800 slurry seal

1800-2303 transition (surveyed in 1990)
2303-2806 GPS site (surveyed in 1990)
2806-3008 transition (surveyed in 1990)

3008-3108 chip seal (surveyed in 1990 before chip seal)
3108-3608 SPS 48H350 chip seal
3608-3708 chip seal
3708 end

3) US Highway 190, GPS Site

Surveyed in the right wheelpath and center of the outside lane, and in the center of the inside lane.

Begins 500 feet before GPS section
0-500 transition
500-1000 GPS Section 483689
1000-1500 transition

For the purposes of this report, the following terminology represents the sections that have been individually analyzed:

Section	Highway	Footage	Description
		Run 1	
SH30-1	SH30	0-1500	GPS Section
SH30-2	SH30	1250-2250	Thin Overlay
SH30-3	SH30	2000-3000	Slurry Seal
		Run 2	
SH30-4	SH30	250-1250	
SH105-1	SH105	1-1000	Thin Overlay
SH105-2	SH105	1001-2000	Slurry Seal
SH105-3	SH105	1800-3300	GPS & Chip Seal
SH105-4	SH105	2750-3750	Chip Seal
US190-R	US190	0-1500	Right Wheelpath
US190-C	US190	0-1500	Centerline
US190-I	US190	0-1500	Inside Lane

Figures 2 and 3 show photographs of the thin overlay and slurry seal pavement sections on SH30. Figure 4 shows the ground truth testing on US 190; the two layers of asphalt and cement stabilized base are clearly visible.

Figure 2. Photograph Showing Thin Overlay on SH 30.

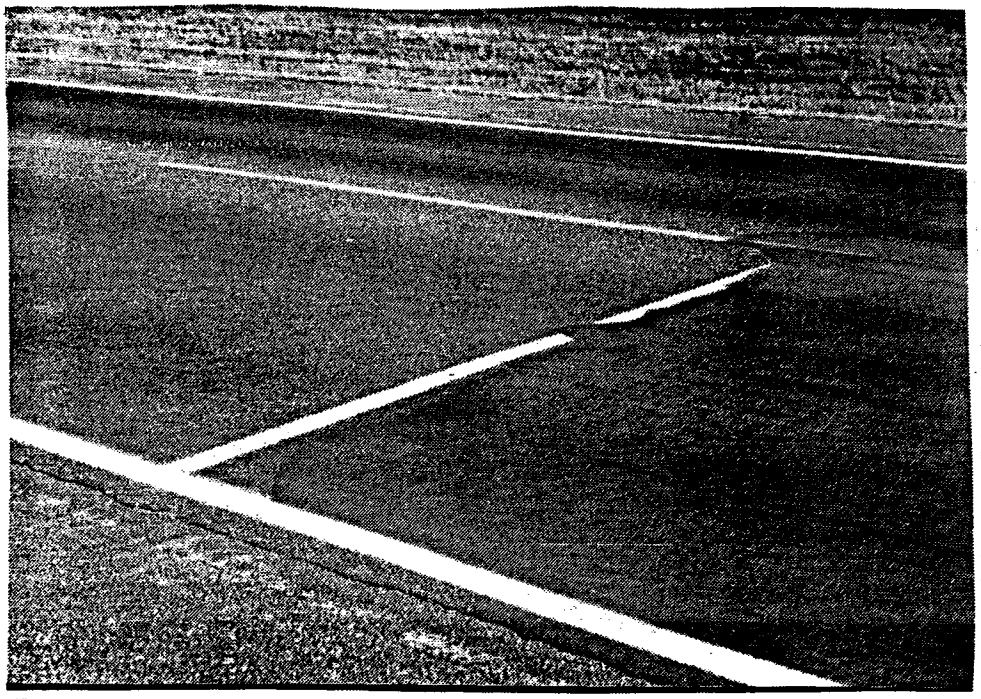

Figure 3. Photograph Showing Slurry Seal.

Figure 4. Ground Truth Testing on US 190 showing two asphalt layers and stabilized base.

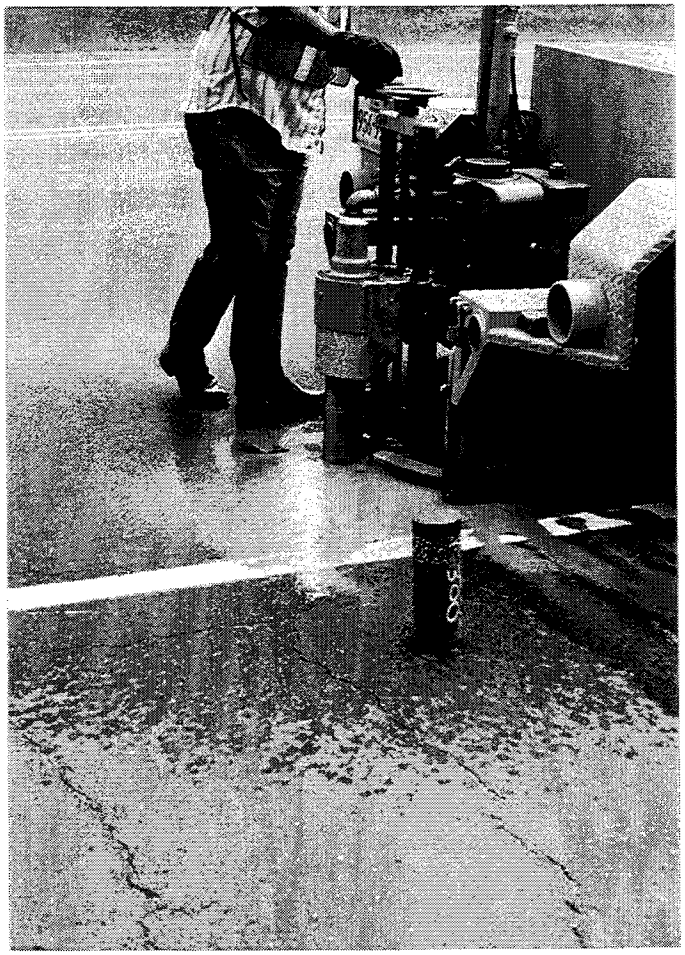

Figure 4. Ground Truth Testing on US 190 showing two asphalt layers and stabilized base.

CHAPTER 4
RADAR DATA COLLECTION

4.1 Equipment and Data Characteristics

Radar data for this project was collected using TTI's Penetradar PS-24 horn antenna radar system suspended above the pavement from the front of a TTI van (see photo in Figure 5). The characteristics of the radar data produced by this system are very similar to those of the Pulse Radar system used in the 1990 study. The system produces 50 waveforms per second. The data was digitized and stored using a data acquisition system developed by TTI. This system utilized a Data Translation analog/digital conversion board housed in a Compaq 33 MHz, 386 computer. Each waveform was digitized into 1024, 12 bit data points, as compared with the 252 point, 8 bit digitization provided by the RDAS system used with the Pulse Radar system. Figure 6 shows the data acquisition equipment setup in the TTI van.

Distance data was collected and recorded using a DMI connected to the transmission of the survey vehicle. The distance data was transmitted from the DMI via the computer serial port, and stored as the 1024'th data point of the waveform. Due to the slow data transmission through the serial port, only one in every 10 waveforms received updated distance data. Later, continuous distance data was generated by linear interpolation.

4.2 Calibration Tests

A series of calibration tests were carried out as part of each field survey. These calibrations are: metal plate reflection, time calibration, and air reflection. In addition to these site calibrations, an overall calibration of the radar system to characterize the radar reflection vs. antenna height was carried out in the TTI Radar research laboratory. As described later, this "height function" was subsequently used to improve the calculation of the asphalt surface dielectric constant; it accounts for any antenna bounce as it travels down the highway.

Figure 5. Photograph on Penetradar Equipment on Van.

Figure 6. Photograph of Equipment in Van.

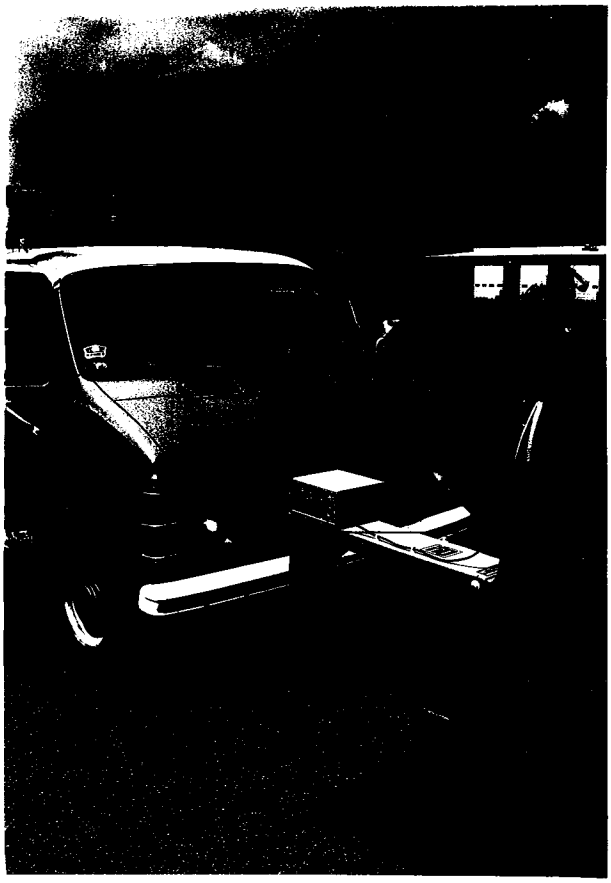

Figure 5. Photograph on Penetradar Equipment on Van.

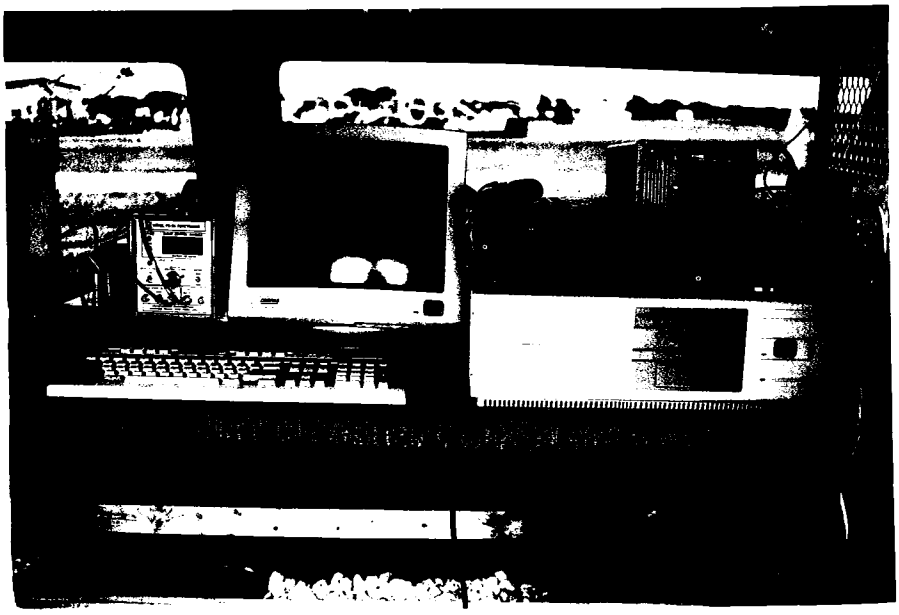

Figure 6. Photograph of Equipment in Van.

The metal plate reflection characterizes the shape of the antenna transmit pulse and the amplitude for that particular antenna height. This measured shape is subsequently used in processing where the surface and subsurface layer reflections are subtracted out to reveal thin layers. The amplitude is used to compute the dielectric constant of the asphalt. Previous work, however, has shown that the height of the antenna varies during the survey from that which existed during the plate test, and the plate amplitude is very sensitive to antenna height. This observation led to the development of the antenna height function calibration, which is described in further detail in Section 6.

The time calibration test measures the radar pulse travel time in air between two metal plates, and compares the measured time to its theoretical value. Time calibration tests of the PS-24 system showed that the "radar" time was 9.5% higher than what the actual time should be. This factor was consistent from test to test. Based on this observation, all radar time was reduced by this factor of 0.92 prior to any data display, analysis and calculations.

The air reflection test was carried out by rotating the antenna so that it pointed up towards the sky, and measuring the response. This "air reflection" data represents the internal reflection of the antenna system, which is inherent to the antenna and its immediate surroundings, and should be constant throughout the survey. The air reflection has no relationship to the pavement condition and can produce some distortion on the pavement data. Recording the air reflection allows for an analysis in which it is removed (subtracted) from the data, thus improving the quality of the data.

4.3 Survey Procedures

Each site was surveyed by first identifying a start location, and then measuring known distances with a survey wheel. For the SHRP sites, the surveys generally began 500 ft. before the beginning of the GPS or SPS section. This location was sometimes already marked on the pavement, but in all cases it was checked or measured with a survey wheel. A metal plate was laid down on the pavement at the beginning and end of each test section to provide beginning and end markers in the radar data.

During the radar survey, the vehicle was operated at approximately 10 mph (15 ft./sec.). This speed was selected to coordinate with the data acquisition system which was set up to acquire 17 scans per second, or approximately one scan per foot. The acquisition rate could have been increased to 50 scans per second, but there was no need to collect what was believed to be an excessive amount of data. All surveys were accompanied by a videolog of the pavement surface. In the current data collection system the DMI is recorded in both the GPR trace and on the video image. This log is later used to correlate radar events with possible pavement surface conditions.

CHAPTER 5
RADAR DATA ANALYSIS

5.1 Data Analysis Principles and Software

The data generated, as described above, was analyzed to calculate pavement layer thicknesses and dielectric constants using INFRASENSE's PAVLAYER software. PAVLAYER (PAVment LAYer Evaluation using Radar) is a menu driven system which implements a variety of analysis alternatives in response to different radar data characteristics. The software utilizes the principles and equations presented in Maser and Scullion, 1991. The pavement layer thicknesses and properties are calculated by measuring the amplitude and arrival times of the waveform peaks corresponding to reflections from the layer interfaces. The dielectric constant of a pavement layer, relative to the previous layer, may be calculated by measuring the amplitude of the waveform peaks from the top and bottom of the layer. The travel time of the transmit pulse within a layer in conjunction with its dielectric constant determines the layer thickness. The reader is referred to the above references for further details regarding the methods of analysis.

New features of the analysis which have not been previously reported are its capability to: (1) separate reflections from overlapping layers; (2) internally compute the incident amplitude onto the pavement surface (i.e., the "plate reflection") directly from radar data to account for antenna bounce; (3) remove the internal radar system reflection. Methods for evaluation and implementation of these capabilities are presented in Chung and Carter, 1989.

PAVLAYER is capable of implementing a number of different analysis alternatives depending on the situation and the interest of the user. The analysis procedure detects amplitude and arrival time of peaks or preceding troughs, with end reflection removed and surface reflection removed, and the possible removal of one subsurface reflector. Plate reflection amplitude is calculated from the data based on predefined height function. Pavement systems requiring the computation of the thickness of more than two layers are analyzed by multiple analyses, with successive analyses computing the thicknesses of the deeper layers.

5.2 Project Specific Software Modifications

Prior to implementing the PAVLAYER analysis, some modifications were made to adapt the TTI data format to the PAVLAYER software. The PAVLAYER software was modified to recognize the 12 bit radar data and the method of distance encoding produced by the TTI data acquisition system. Two additional programs were written to convert the TTI data to a format compatible to PAVLAYER: one to subsample the data by a factor of four, and one to interpolate the distance data so that every waveform had distance information in the last data point.

As noted earlier, an antenna height function had to be established in order to continuously compute plate reflection amplitudes with antenna height variations. The initial calibration data was collected in the TTI lab by continuously raising and lowering a metal plate with the antenna mounted in a fixed position (see Figure 7). The range of heights was 8 to 14 inches, which represented the typical height range which may be encountered in the field. At each height the amplitude of reflection was measured. Since metal plate reflections do not exactly replicate reflections from a pavement, this height function was calibrated to using 1 core taken in 1990 from the SH30 site. This calibrated height function was encoded into the software.

5.3 Example of Layer Thickness Calculation

Figure 8 shows a typical GPR trace from a test box sample constructed in the TTI laboratory. The box contained 6 inches of asphalt over a 6 inch granular base. The software analysis system permits the user to specify windows for determining amplitudes and time delays. From Figure 8 the asphalt dielectric (ϵ_{ac}) and layer thickness (h_{ac}) is calculated as follows,

$$\sqrt{\epsilon_{ac}} = \frac{A_m + A_o}{A_m - A_o} = \frac{12.92 + 5.25}{12.92 - 5.25} = 2.369$$

$$h_{ac} = \frac{c\ \Delta t}{\sqrt{\epsilon_{ac}}} = \frac{5.36 \times 2.64}{2.369} = 5.97 \text{ inches}$$

where A_m = amplitude of reflection from metal plate,

A_o = amplitude of reflection from asphalt surface,

Δt = time delay between peaks (nanoseconds),

c = constant.

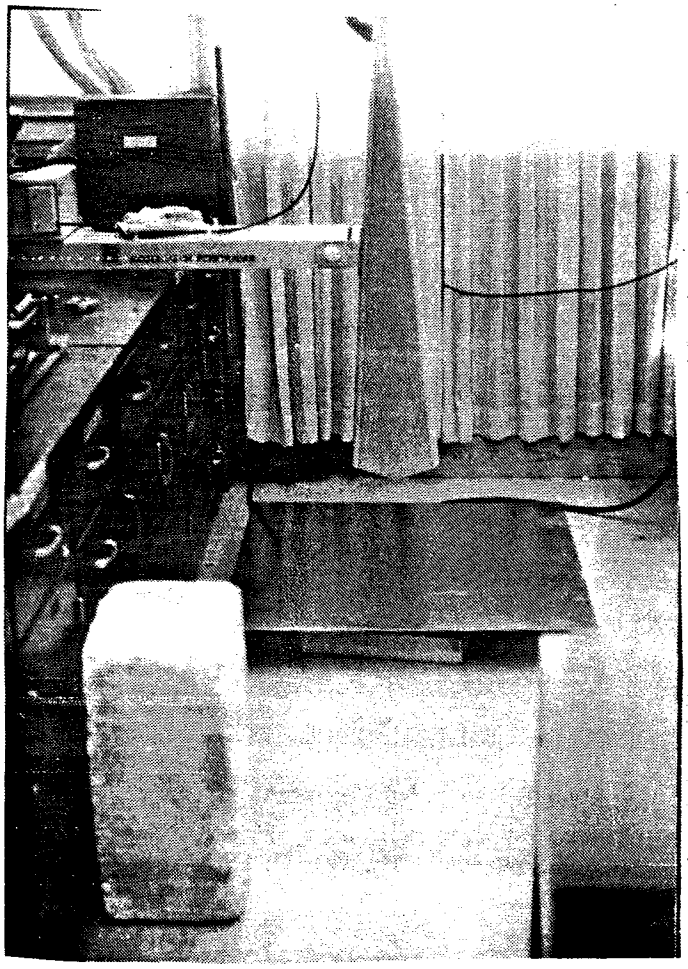

Figure 7. Photograph of Lab Height Calibration Test.

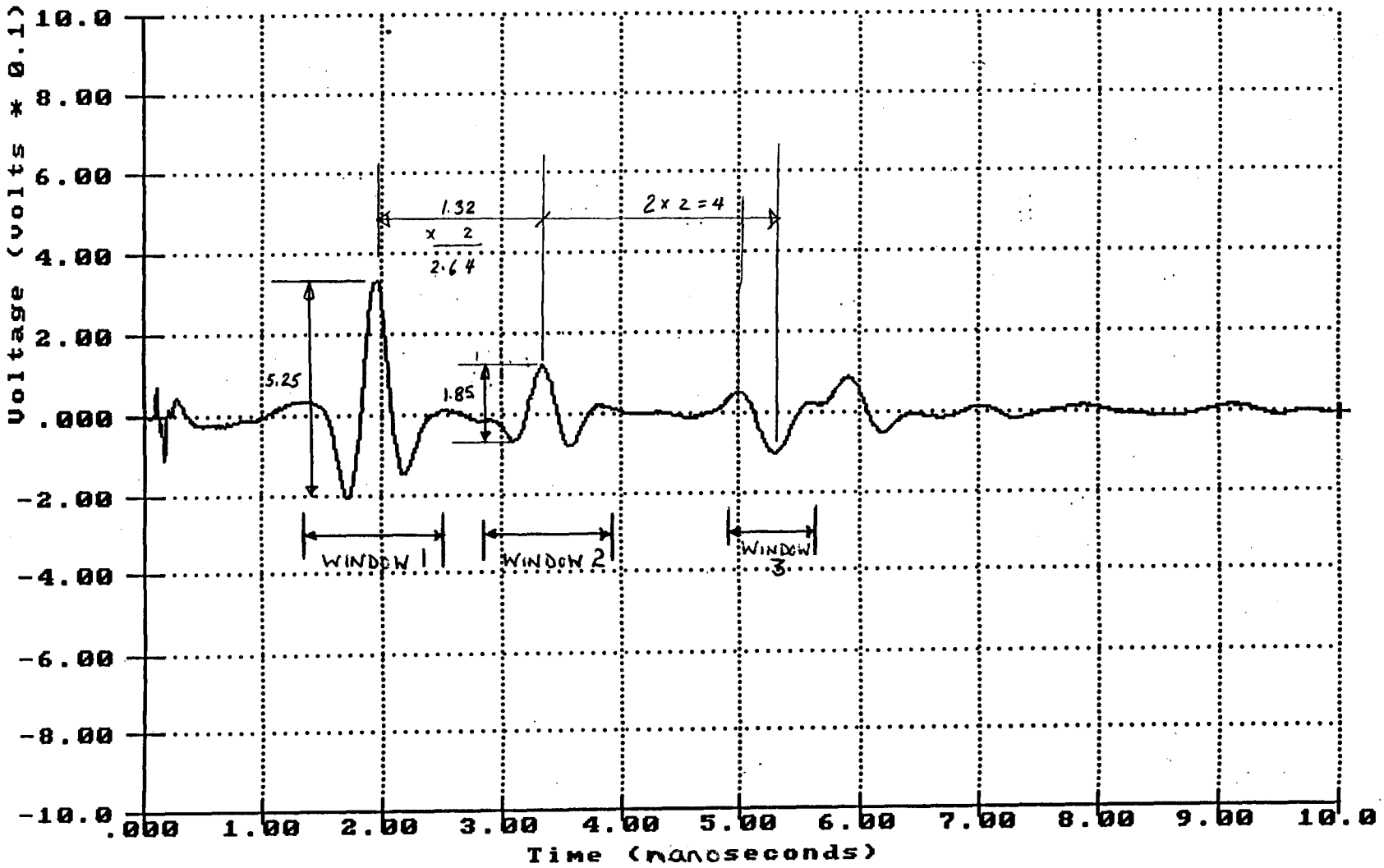

Figure 8. Typical GPR Traces from a Control Box Containing Six Inches of Asphalt Over a Six Inch Granular Base. The "WINDOWS" are User Specified to Permit Peak Detection and Layer Thickness Calculation

CHAPTER 6
GROUND TRUTH

Ground truth was obtained for asphalt and base layer thicknesses. The asphalt layer thickness ground truth was obtained using 6 inch diameter wet cores. Coring was also used for the thickness evaluation of the cemented base on US190. Granular and treated base thickness evaluation was carried out using a grooved cylindrical sleeve. The sleeve is placed in the corehole at the top of the base. It is then driven through the base into the subgrade. The base and subgrade material remained embedded in the groove, and the boundary could be observed when the cylinder was removed. The location of this boundary provided a measure of the base thickness.

CHAPTER 7
RESULTS

7.1 Comparison of Repeat Surveys

In this section, results are presented comparing data collected using the Penetradar PS-24 system and data collected by the Pulse Radar R-II system in the 1990 study. The 1990 study also included a repeat survey, the results of which are also included where applicable. All of these comparisons are carried out using the same data analysis software, with adaptations for the different equipment as described earlier. Results are also presented comparing the 1990 analysis of the Pulse R-II data and a repeat analysis of this data using the current generation of PAVLAYER. These comparisons are made possible by the fact that GPS sections on SH30 and SH105, which were surveyed during the 1990 survey, were resurveyed during this 1991 study.

7.1.1 Comparisons for SH30

Figures 9, 10, and 11 show the computation of asphalt and base layer thicknesses using both radar systems. The core data shown in Figure 9 represents coring carried out in both the 1990 study and the current study. In Figure 10, the base thickness "core" ground truth data has been separated for the two studies, since different methods for base thickness evaluation were used. The earlier ground truth base thicknesses were obtained using a Dynamic Cone Penetrometer, the latter with the slotted cone as described earlier.

For asphalt thickness, slight differences appear between the results for the two systems, but nothing significant. The radar data matches the cores very closely for both systems. The primary divergence is in the 7/27/90 R-II survey results. This divergence is due to the fact that the antenna was mounted significantly lower than for the other work (about 12" above the pavement). This height is beyond the linear range of the R-II height function (15 to 20 inches), and results in a slight underestimation of the asphalt dielectric constant (see Figure 11).

For the base thickness, the R-II data matches the ground truth, but the PS-24 data diverges significantly. Examination of the raw data reveals that the base/subgrade reflection for this site is much weaker in

the PS-24 data than the R-II data as will be discussed later. Therefore, it is postulated that the PS-24 error is due to the loss of a significant reflection to track. To explore this hypothesis, the strength of the base/subgrade reflection, normalized by the surface reflection, is plotted for both systems in Figure 12. This plot shows quantitatively that the PS-24 reflections are much lower in amplitude than those from the R-II unit. Comparison of Figure 11 and Figure 12 shows that the PS-24 data is accurate when the normalized base/subgrade amplitude is greater than 0.05. This observation suggests than some threshold amplitude for base/subgrade reflection be used for acceptance of base thickness data. This threshold concept will be discussed in conjunction with other data to be presented in the next sections. There are a number of possible explanations for the differences in the base/subgrade amplitudes for the two radar systems. These include higher frequency content and system clutter in the PS-24, or changes in the actual base/subgrade properties which may have occurred between the 1990 and 1991 surveys. These possibilities will be discussed later.

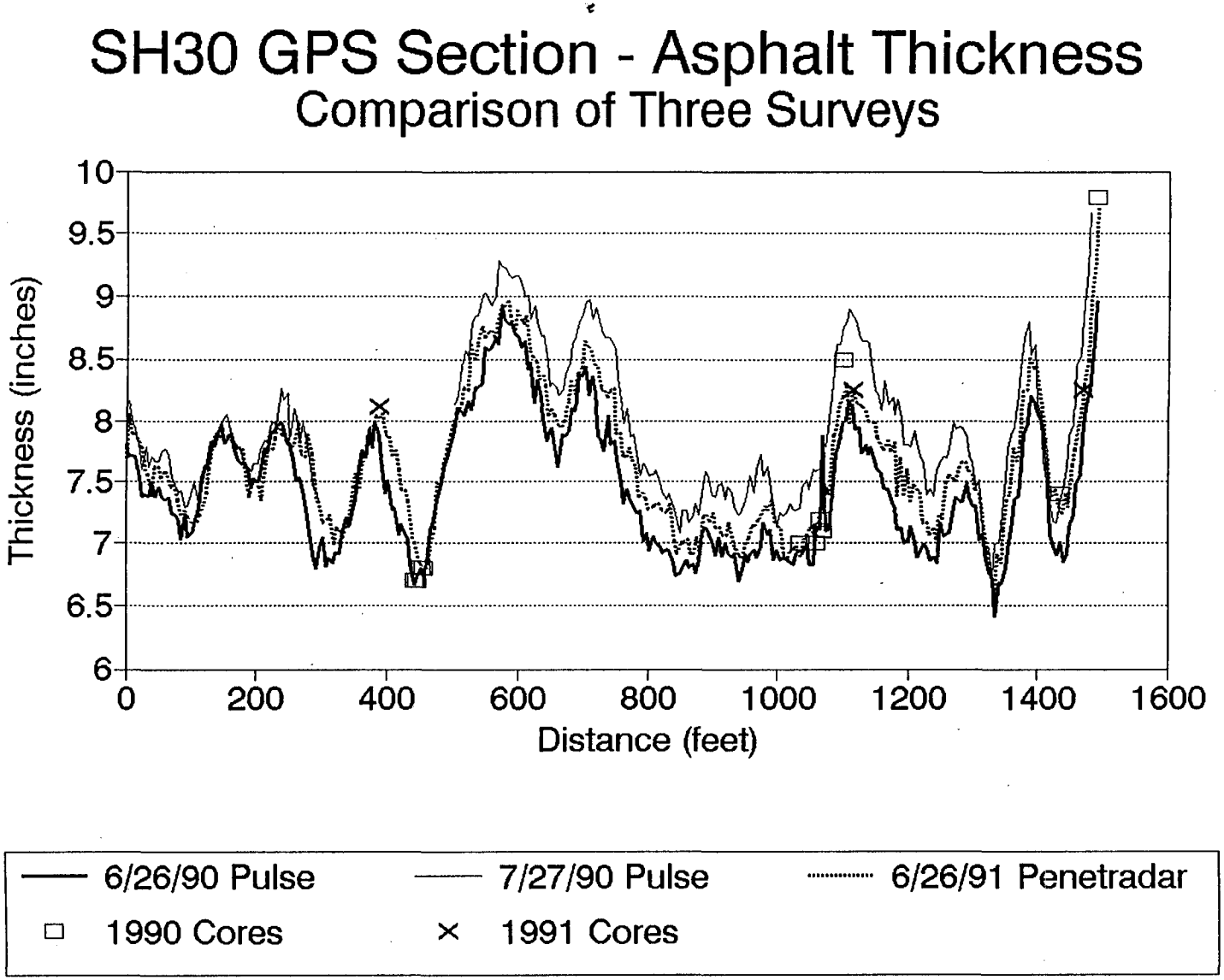

Figure 9. SH 30 GPS Asphalt Thickness.

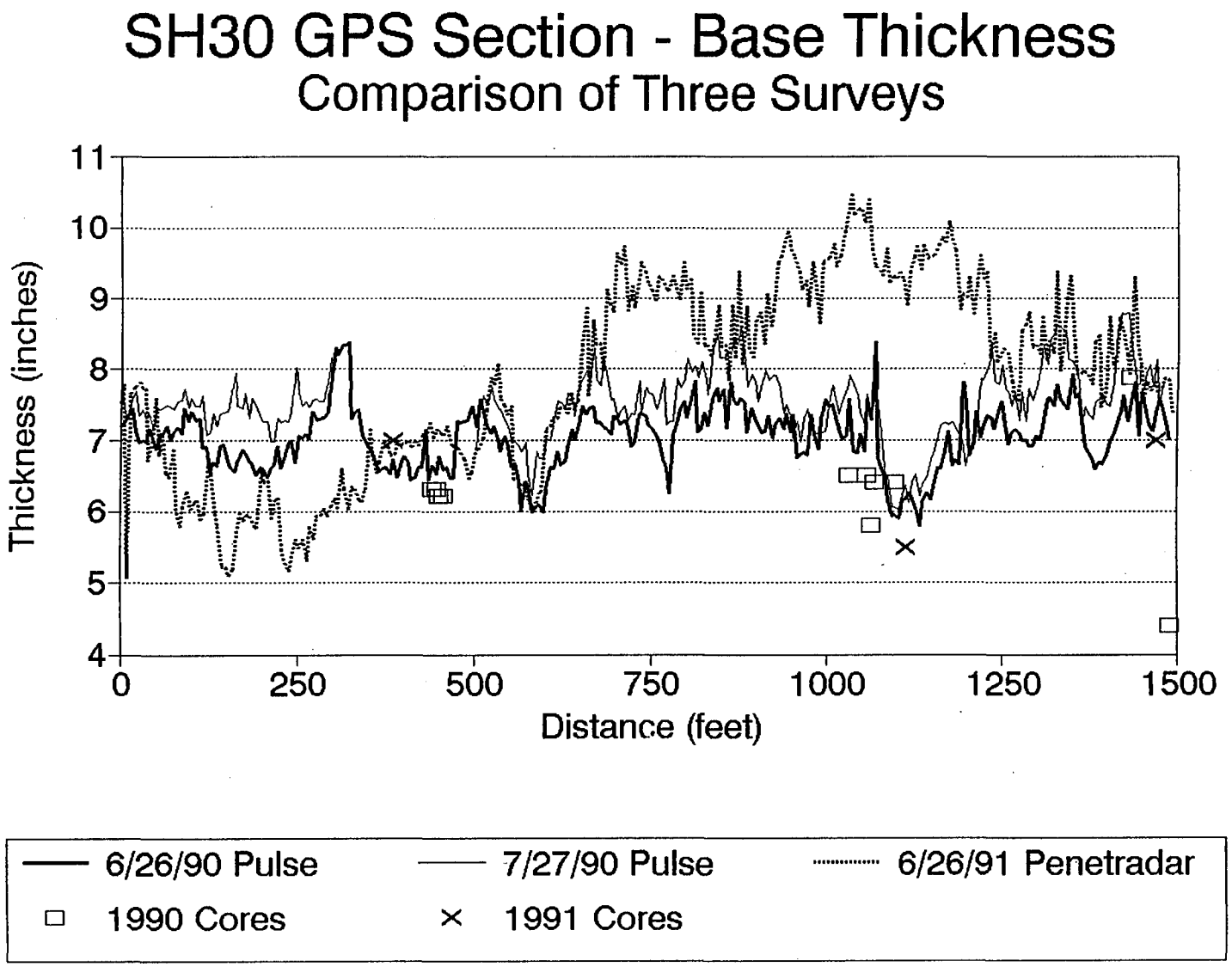

Figure 10. SH 30 GPS Base Thickness.

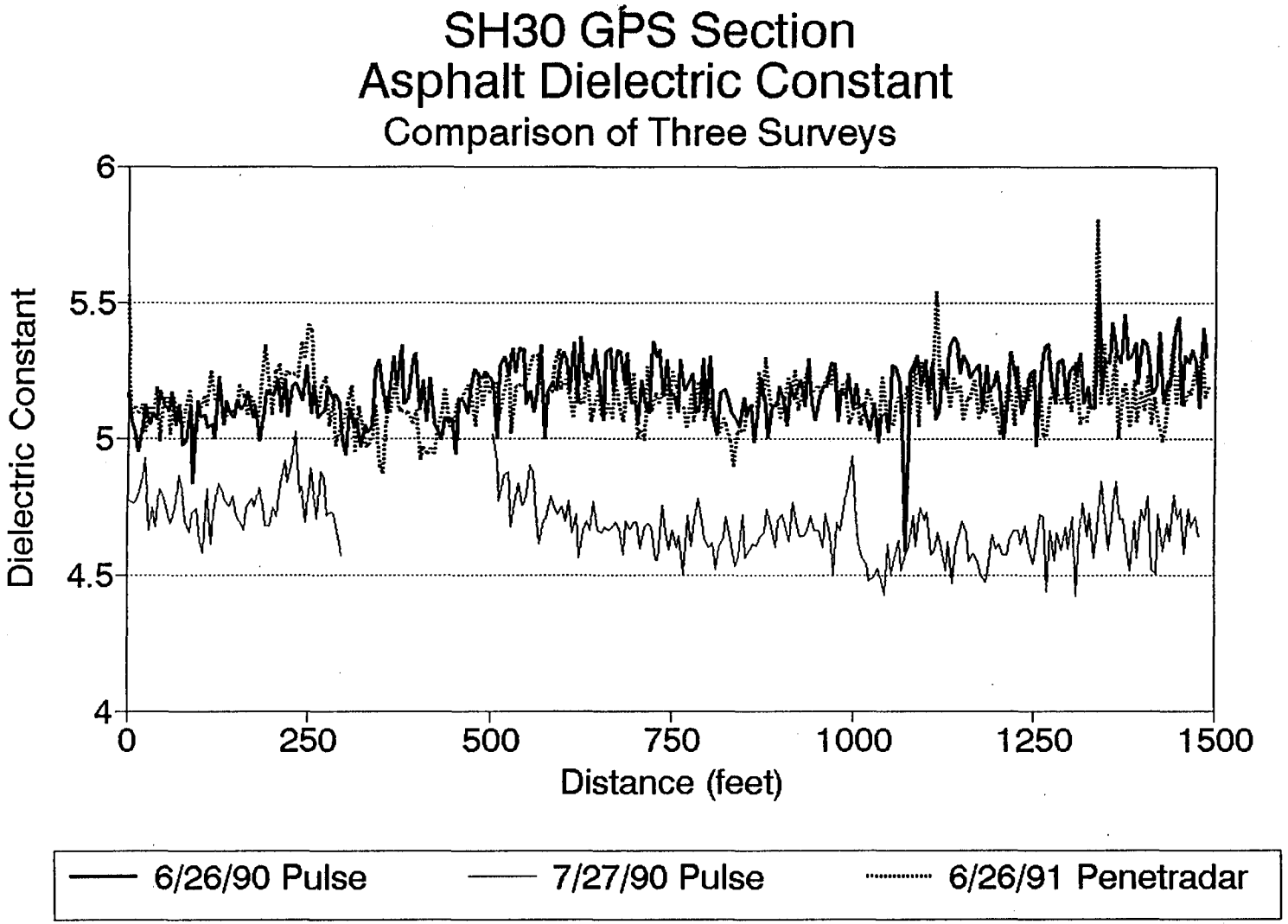

Figure 11. SH 30 GPS Asphalt Dielectric Constant.

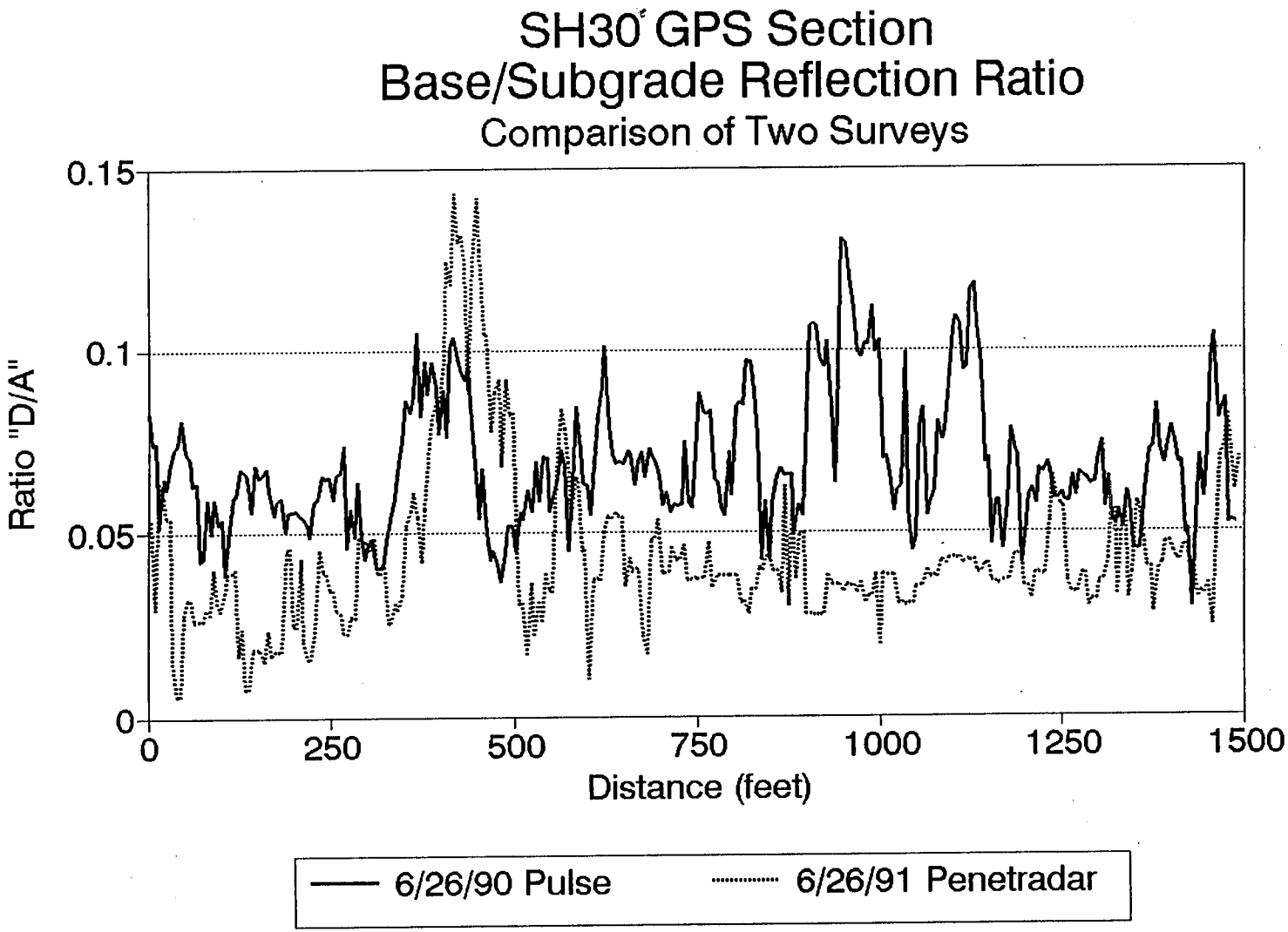

Figure 12. SH 30 GPS Normalized Base/Subgrade Reflection.

7.1.2 Comparisons for SH105

Figure 13 shows analysis layer thickness predictions from the two 1990 R-II surveys and the 1991 PS-24 survey together with the ground truth results. Note that no data was collected between 500 and 1000 feet (the GPS site) during the 7/27/90 R-II survey. The figure shows some differences between the PS-24 and R-II results, with the PS-24 data appearing to be more accurate. Note that these results were produced with an analysis that modelled the two thin asphalt layers. Figure 14 shows the calculated results for the asphalt dielectric constant. Note that the results for the two systems are similar for the first 400 feet, and then diverge for most of the remainder of the section. This result is difficult to explain because there is no systematic difference. It is possible that the reflection from interface between the two asphalt layers is affecting the surface dielectric computation in a way which varies with the top asphalt layer thickness.

Figure 15 shows results for the base thickness. All of the results look similar, except between 300 and 400 feet where the PS-24 results diverge, and between 1300 and 1440 feet, where the 7/27/90 R-II results diverge. The base thickness predictions are reasonably close to the core values, except for the point at 260 feet. Note from the 1990 report that the direct base thickness measurement at this location was made by visual observation in the corehole, rather than with the penetrometer as used at the other locations.

The PS-24 base thickness results diverge from the other results in a region where the normalized base/subgrade amplitude is less than 0.05 (see Figure 16). This observation further supports the concept of a threshold value for acceptance of base thickness data. Note also that overall amplitude of the base/subgrade reflection for the PS-24 data is approximately 25% less than that for the R-II data. The similar reduction observed on the SH 30 data supports the conclusion that the reduced amplitude is related to the antenna and not to changed pavement conditions.

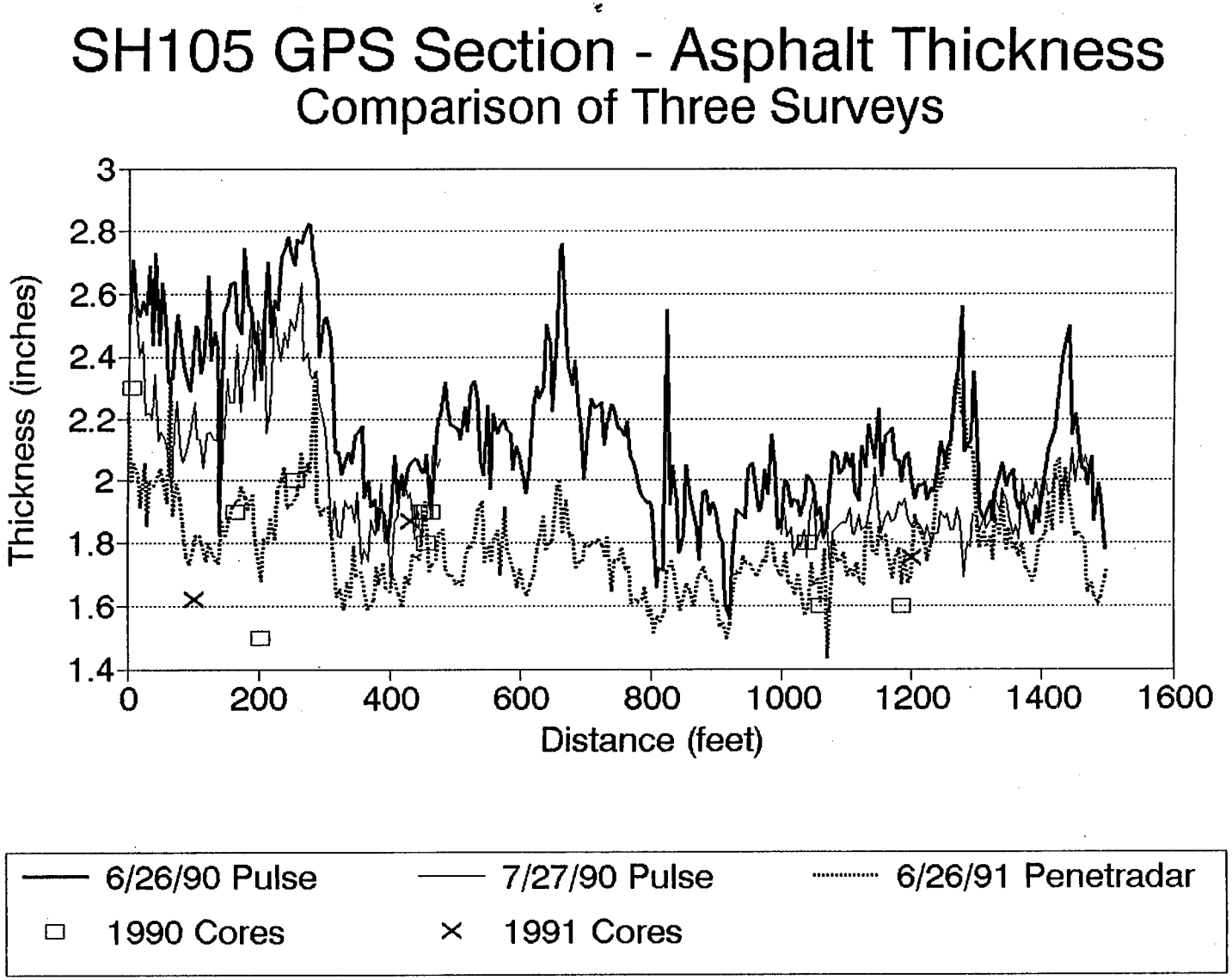

Figure 13. SH 105 GPS Asphalt Thickness.

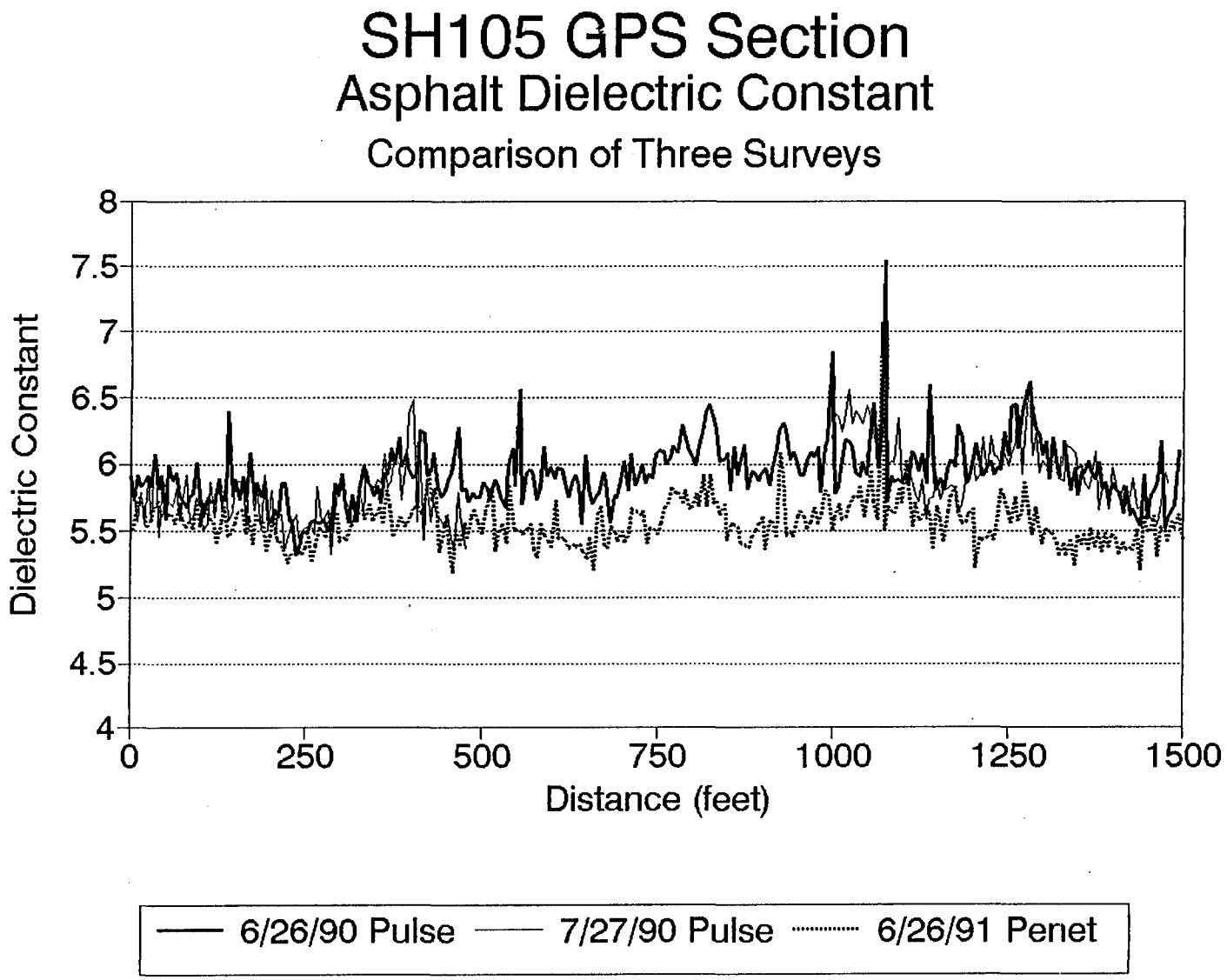

Figure 14. SH 105 GPS Asphalt Dielectric Constant.

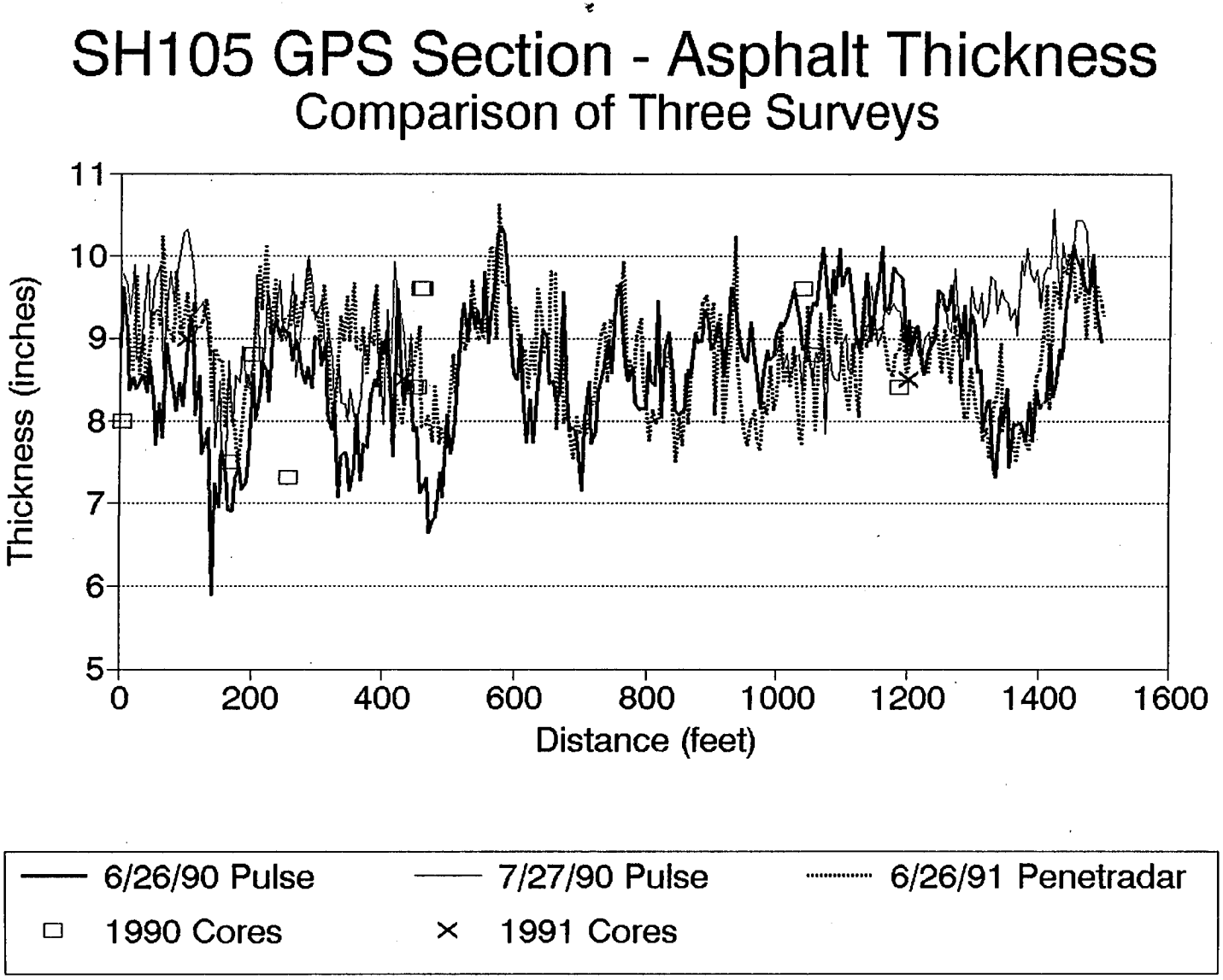

Figure 15. SH 105 GPS Base Thickness.

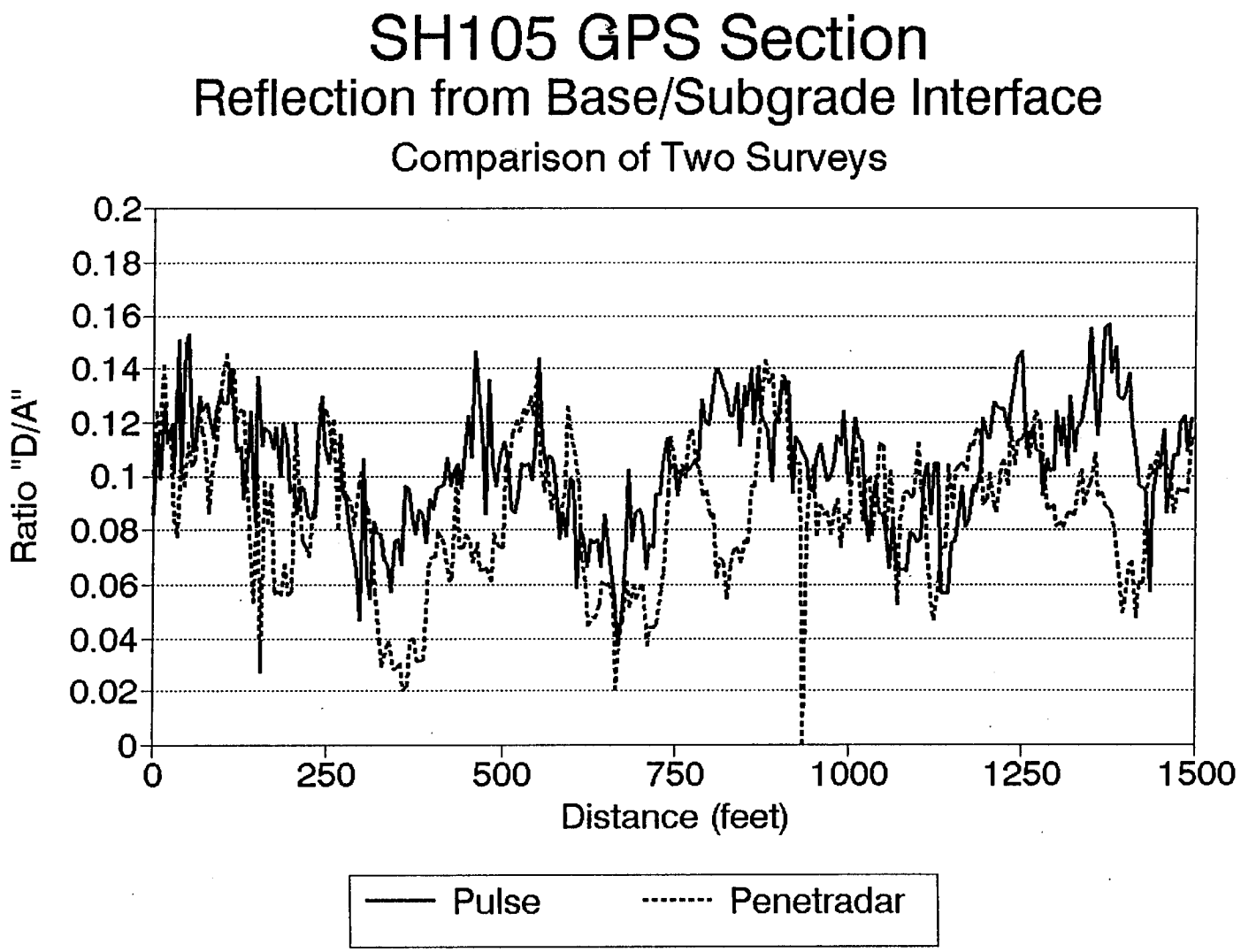

Figure 16. SH 105 GPS Normalized Base/Subgrade Reflection.

7.2 Evaluation of Thin Overlays

Thin overlay sections associated with SPS studies were placed on SH30 and SH105 sections between the 1990 and 1991 surveys. Because of their proximity to the original GPS sections, these overlays provided an excellent opportunity to focus on the influence of the overlay on the radar data. The SH30 overlay section was only 500 feet long, and due to SHRP program restrictions, no cores could be taken in this section. The SH105 section, however, had a 700 foot overlay section, with leading and trailing 100 foot transitions sections in which cores could be taken.

7.2.1 Thin Overlay on SH30

Figure 17 shows a plot of successive raw radar waveforms at the location where the thin overlay begins, the vertical scale is trace number. Figure 18 shows the same plot with the reflection from the asphalt surface removed. This subtraction involves scaling positioning and subtracting the metal plate reflection trace from the field data trace. Note that while the overlay is not apparent in the raw Figure 17 data, it is clearly revealed in the processed Figure 18 data. This method of revealing thin layers provides a means for calculating their thickness. Figure 19 shows the thickness of the overlay vs. distance, together with the dielectric constant of the original pavement surface. Note that the dielectric constant of the original asphalt pavement surface rises from 5.2 before the overlay to about 6.0 in the overlay section. The rise in dielectric of the asphalt could be due to the construction process where the tack coat prevents the evaporation of moisture or related to the temperature difference at the two tests.

Note also that the asphalt dielectric constant between 1580 and 1720 feet, shows numerous location of high values above the baseline value of 6. Experience with similar data (see Section (eg., Fernando and Maser, 1992) suggests that such behavior is characteristic of the interface rather than of the entire layer. Therefore, data processing for layer thicknesses should use the "background" level dielectric constant rather than its local variation. The local variations may possibly be due to moisture trapped between the overlay and the main pavement layer. This behavior is also observed on US190, as discussed later.

In general the layer thicknesses estimated with radar for the thin overlay were very reasonable. The nominal thickness for the SHRP overlay was 1.25 inches. This is very close to the results shown in Figure 19. It appears that the subtraction process holds promise that thin overlays may be accurately measured with these 1 GHz radar systems. This implies that GPR could have potential applications in the area of quality control. Without the subtraction process it was impossible to accurately estimate any layers less than 3 inches thick. In the future thin layer resolution could be improved if the new higher frequency GPR unit, currently under development such as 2.5 GHz, can be improved to match the operational stability of the conventional 1 GHz units.

Figure 20 shows a plot of the total asphalt thickness including overlay and original pavement. Two plots are shown: one in which the overlay has been ignored in the analysis, and one in which the overlay has been specifically computed. The difference in these two calculations is that the one which computes the overlay also computes the higher dielectric constant of the main asphalt layer. The results show that the second analysis produces lower thickness values due to the higher dielectric constants. Due to the lack of available core locations, no verification of these analyses has been made. However, the overlay can be clearly identified and calculated, and that calculation produces different results for total asphalt thickness than an analysis which ignores the overlay. Ignoring the overlay means that the same dielectric will be used to compute total asphalt thickness. This will lead to error if the presence of the overlay can be observed in the data as shown in Figure 18.

7.2.2 Thin Overlay on SH105

SH105 is composed of an original 1" HMAC layer with limestone aggregate covered by a 1" thick overlay made from an iron ore aggregate. The SPS thin overlay section, therefore, represents a third layer. Earlier, in section 7.1.2, it was noted that the two layer asphalt model produced good results for asphalt and base layer thickness. The influence of this third asphalt layer on the analysis results and their correlation to core values is investigated below.

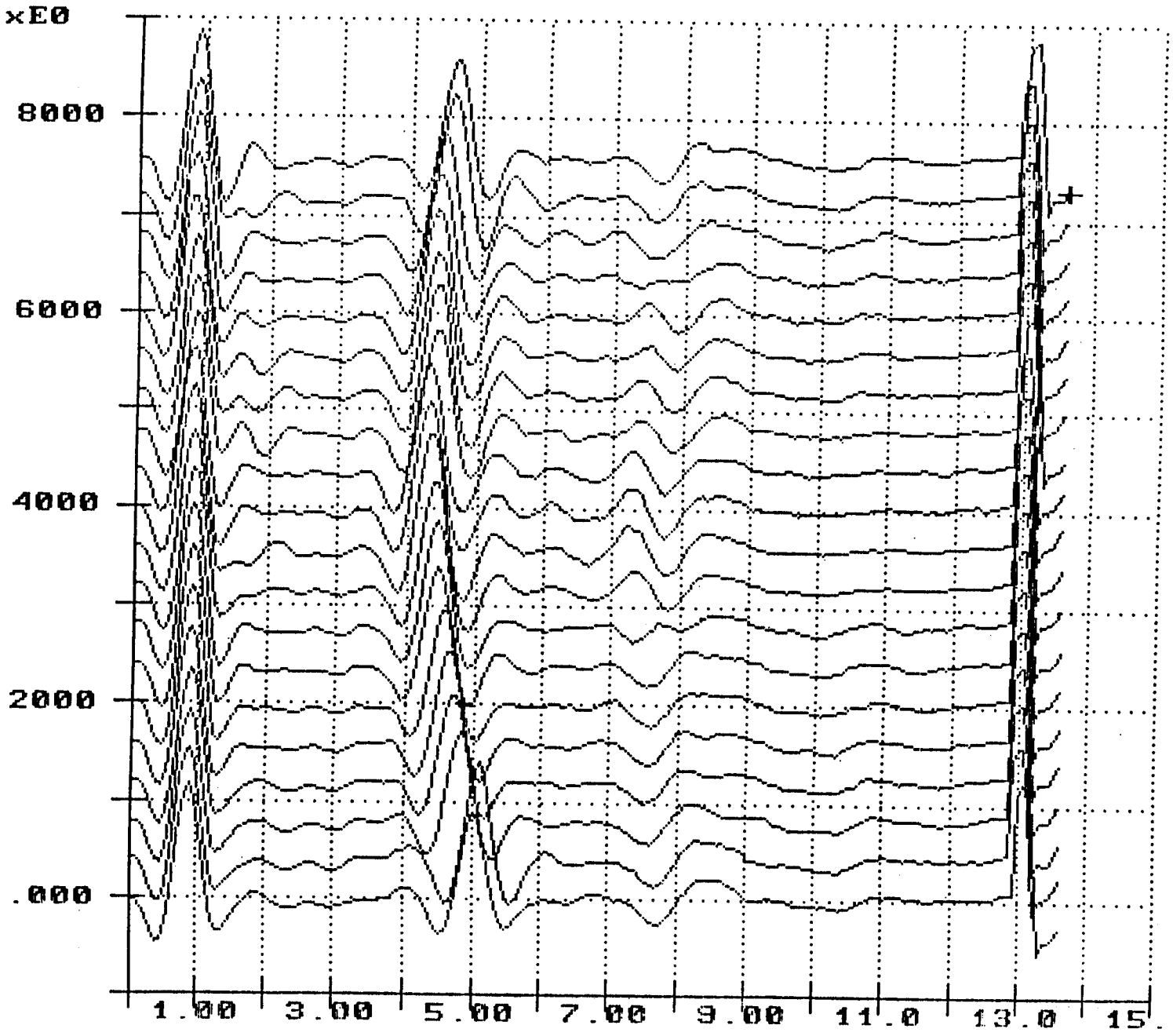

Figure 17. Raw Waveforms at the Beginning of SH 30 Thin Overlay.

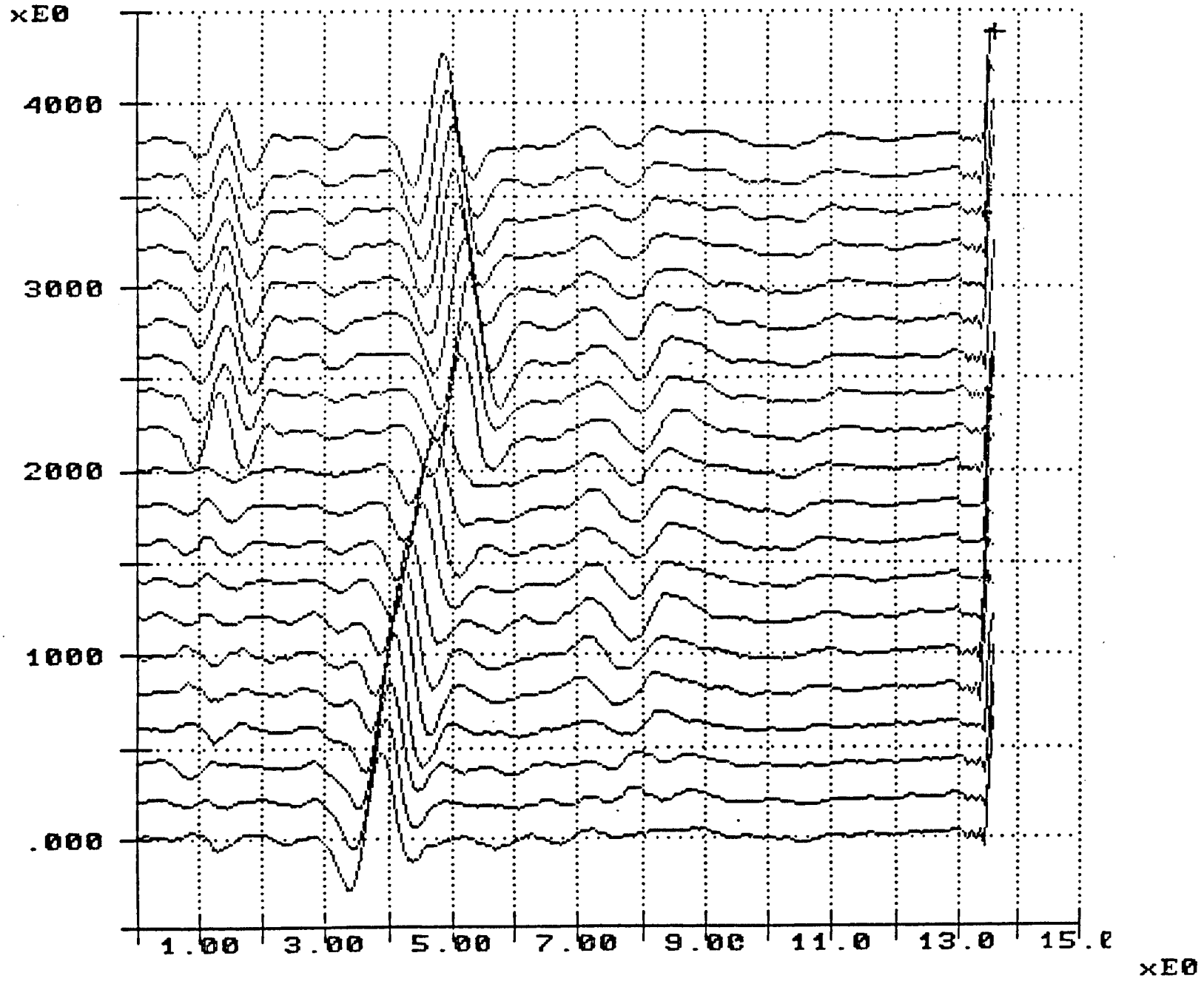

Figure 18. Waveforms at the Beginning of SH 30 Overlay Processed by Removing the Surface Reflection.

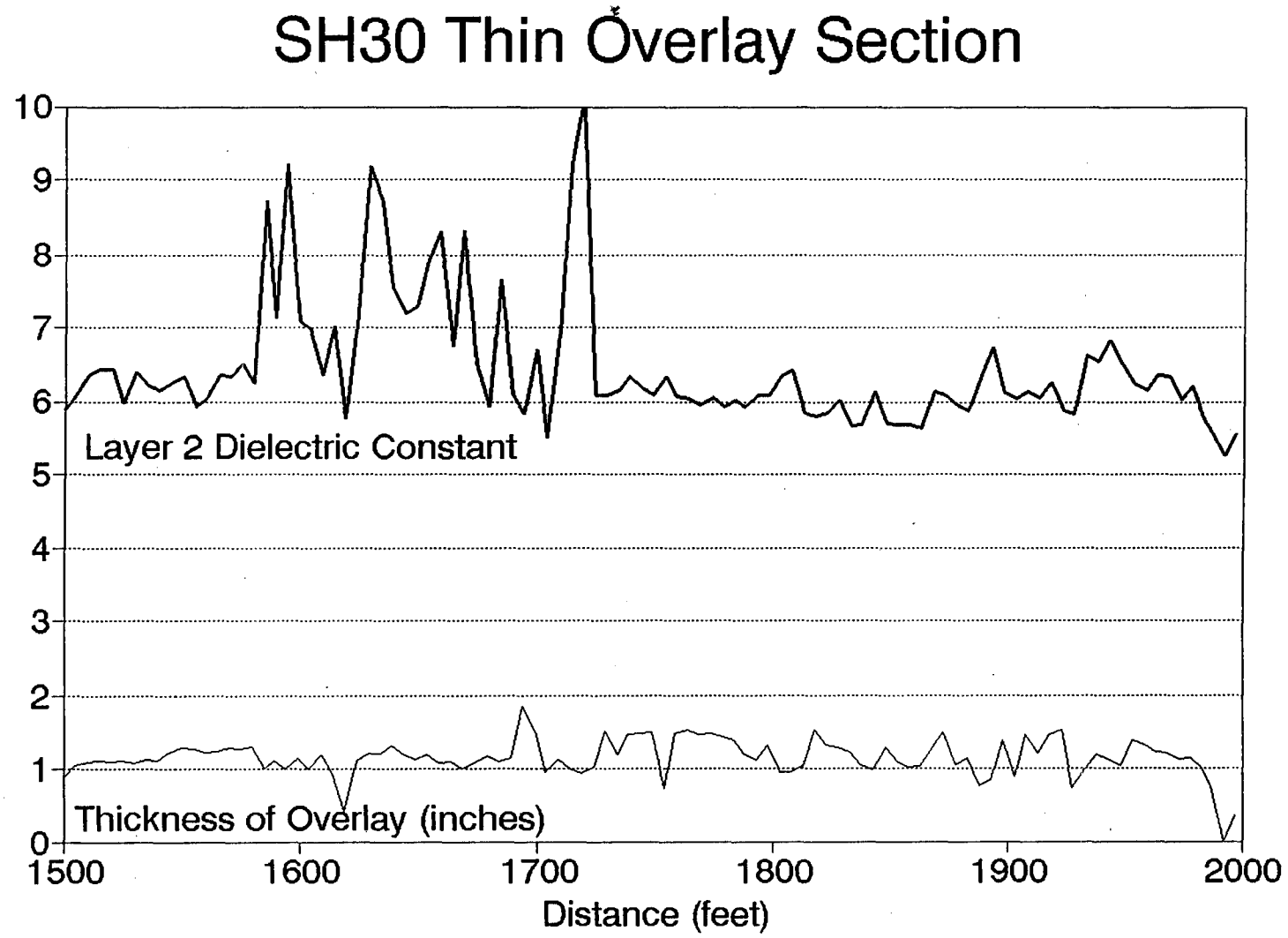

Figure 19. SH 30: Thickness of Overlay and Dielectric Constant of Original Pavement.

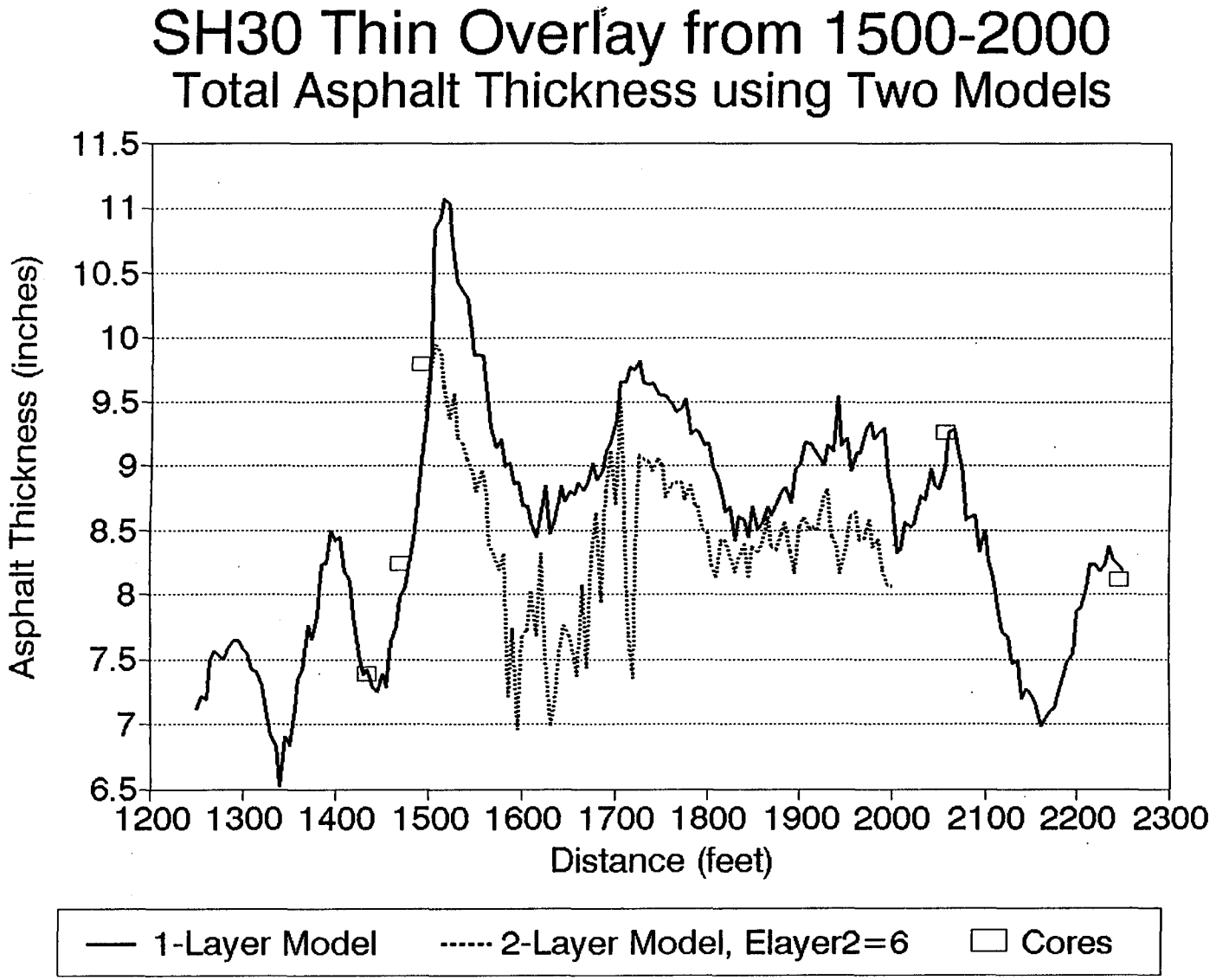

Figure 20. SH 30 Total Asphalt Thickness in Overlay Section.

Figure 21 shows the raw radar waveforms at the transition from the original pavement to the overlay section, and Figure 22 shows the same data with the surface reflection removed. The first peak at approximately 1.8 ns is from the second asphalt layer; the peak at 7.5 ns is from the base/subgrade interface. At approximately trace number 2000, a third asphalt peak is seen which is caused by the thin overlay. Figure 23 shows the processed thickness results using both a one and a two-layer model for the asphalt together with ground truth results. The Figure shows that the two-layer model produces fairly accurate results for the asphalt, while the accuracy is slightly degraded using a one-layer model.

Figure 24 shows the asphalt dielectric constant for a 1000 foot section including the thin overlay. Note that the asphalt dielectric constant drops from approximately 6 in the original section to 5 in the overlay section. This change reflects the change in material properties between the original overlay and the SPS overlay, due possibly to the differences in aggregate types or mix density.

Figure 25 shows the base dielectric constant for the same section as Figure 24. Note that the calculated base dielectric constant drops significantly from a value of about 12 in the original section to a value of 8 in the overlay section. One possibility is that the new overlay has prevented moisture infiltration, and the dielectric constant of the limestone base has consequently dropped. A more likely explanation, however, is that the one- and two-layer models do not adequately represent the three-layer asphalt system, and that this inadequacy shows up in the base. The lack of a model for the third asphalt layer would naturally lead to a lower base dielectric constant, since one layer in the progression on increasing dielectric constants has been missed.

Figure 26 confirms the latter hypothesis by comparing the base thickness predictions using the one- and two-layer models, and using a third two-layer model in which the base dielectric constant is set to 12. The results show that accurate base thickness calculations can be made by setting the base dielectric constant to what it has been determined to be in the two-layer sections. They also show that by not recognizing this third layer, the base thickness calculations are overestimated by at least 20%.

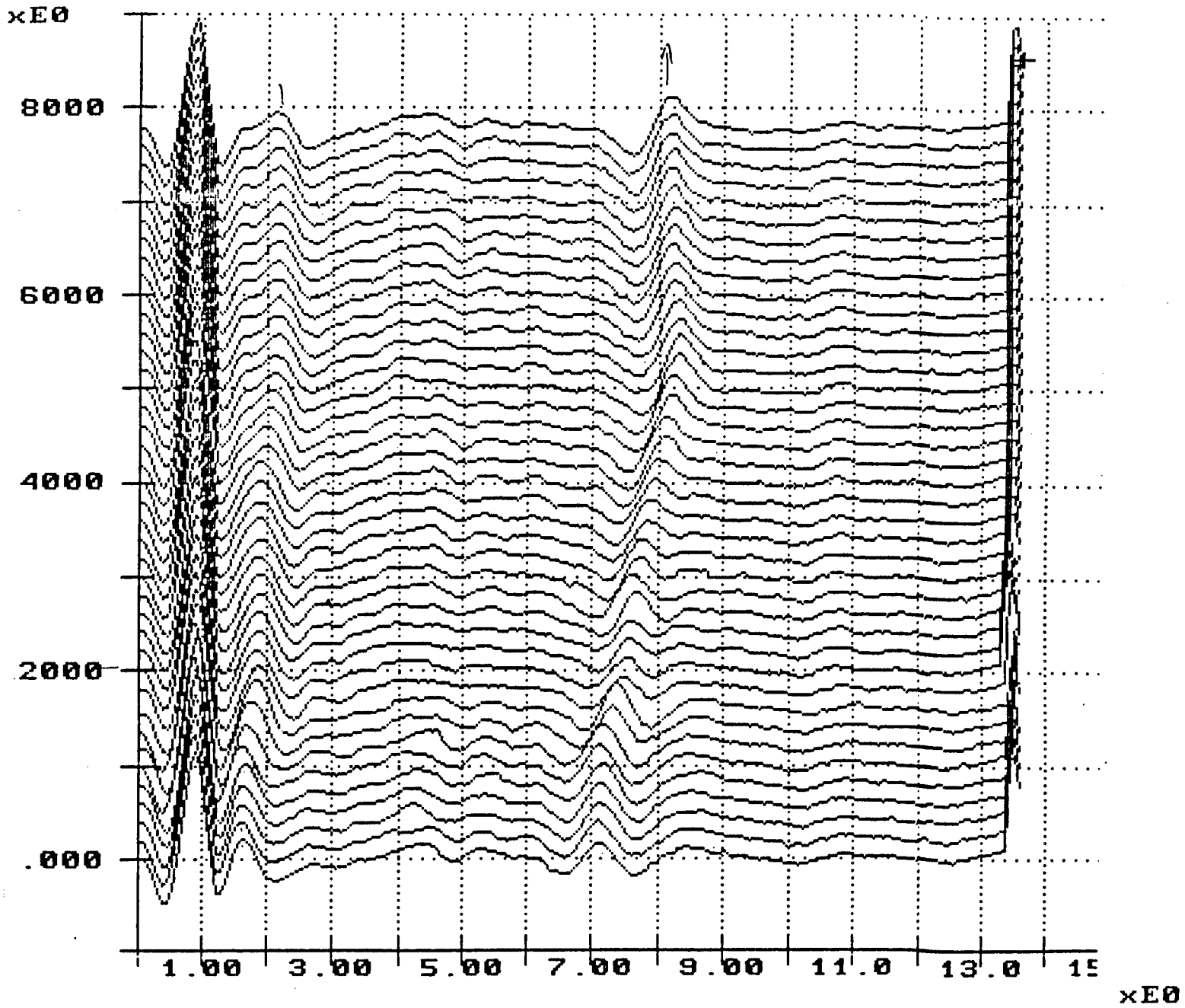

Figure 21. Raw Waveforms at the Beginning of SH 105 Thin Overlay.

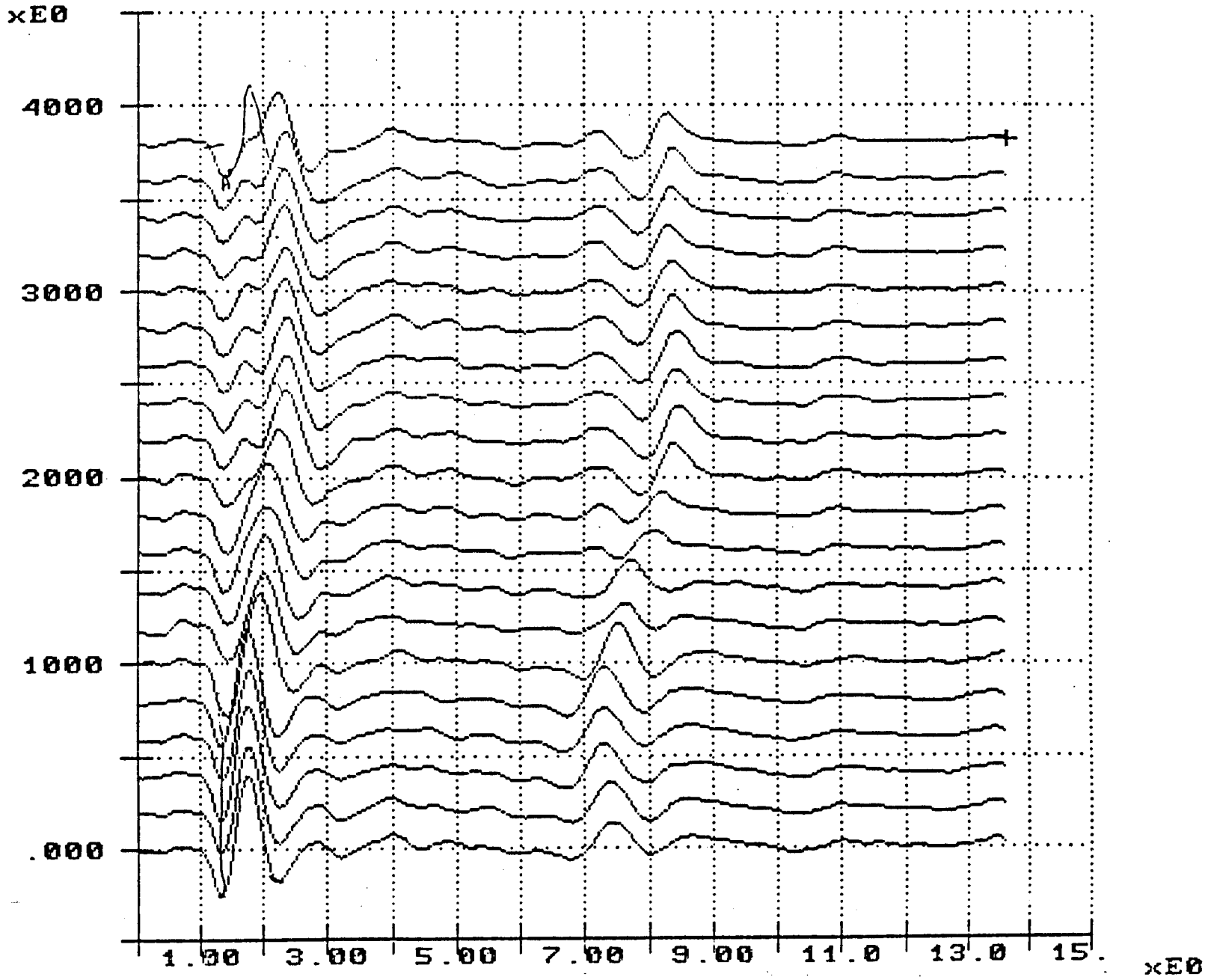

Figure 22. Waveforms at the Beginning of SH 105 Thin Overlay Processed by Removing the Surface Reflection.

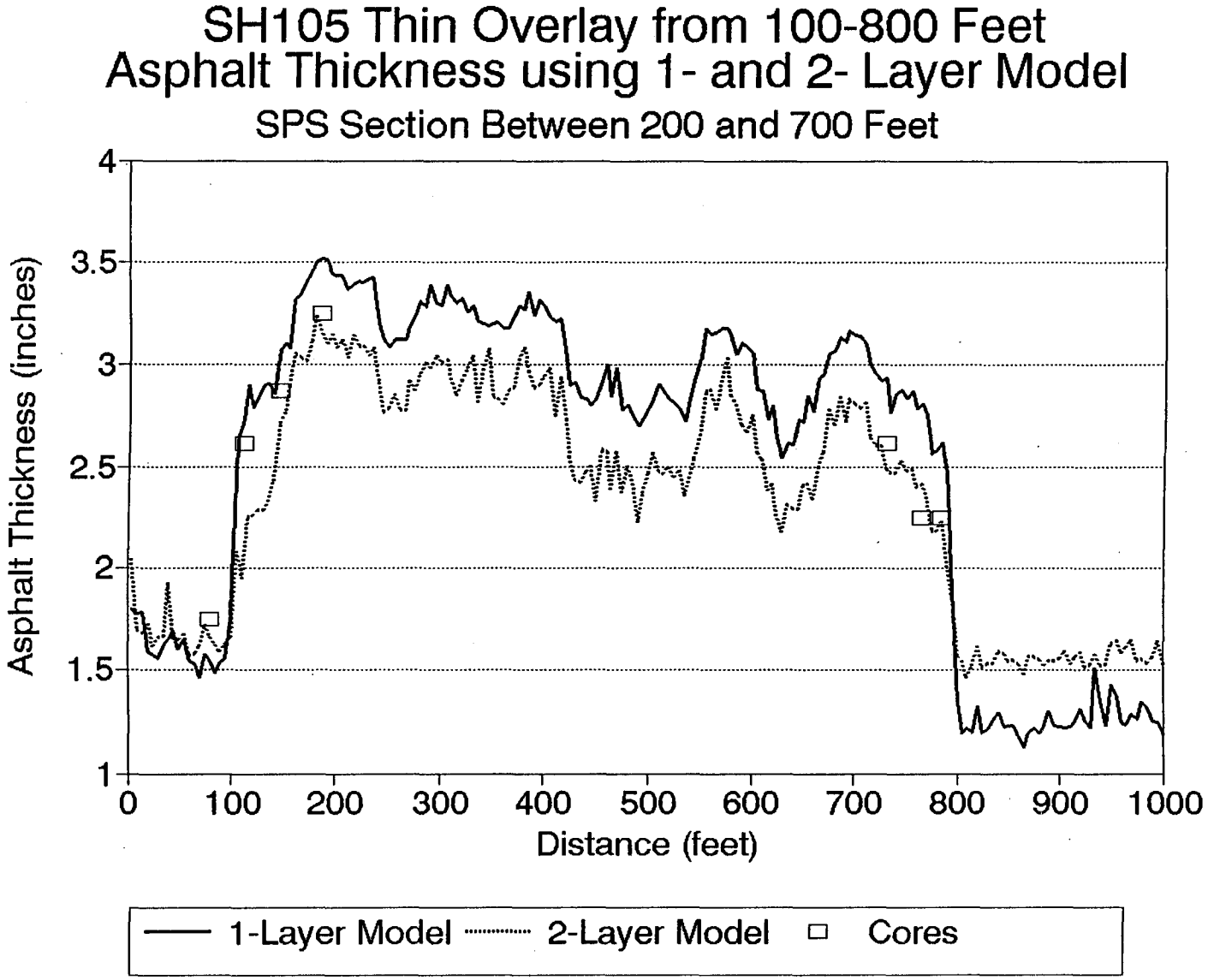

Figure 23. SH 105 Total Asphalt Thickness in the Overlay Section.

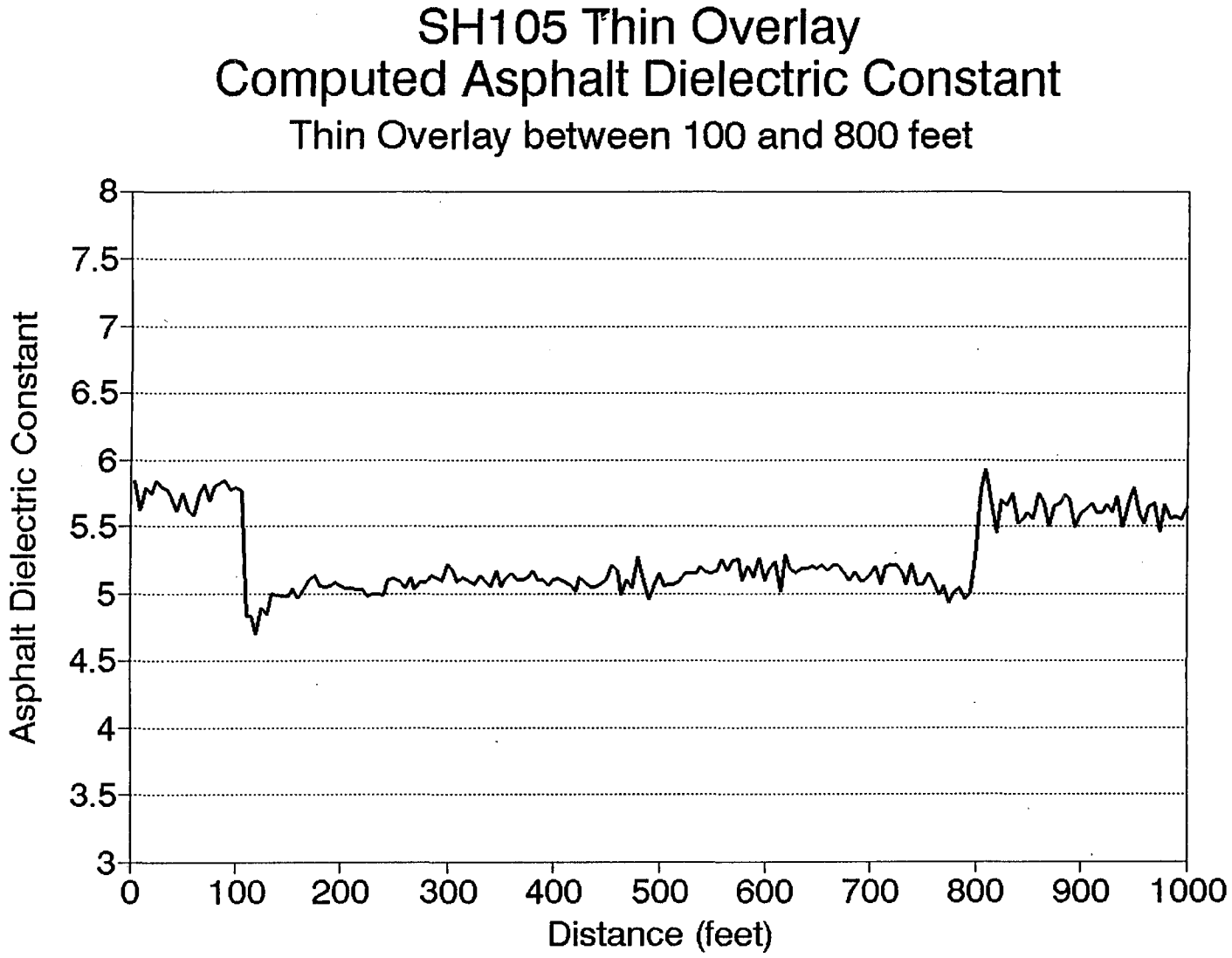

Figure 24. SH 105 Asphalt Dielectric Constant in the Overlay Section.

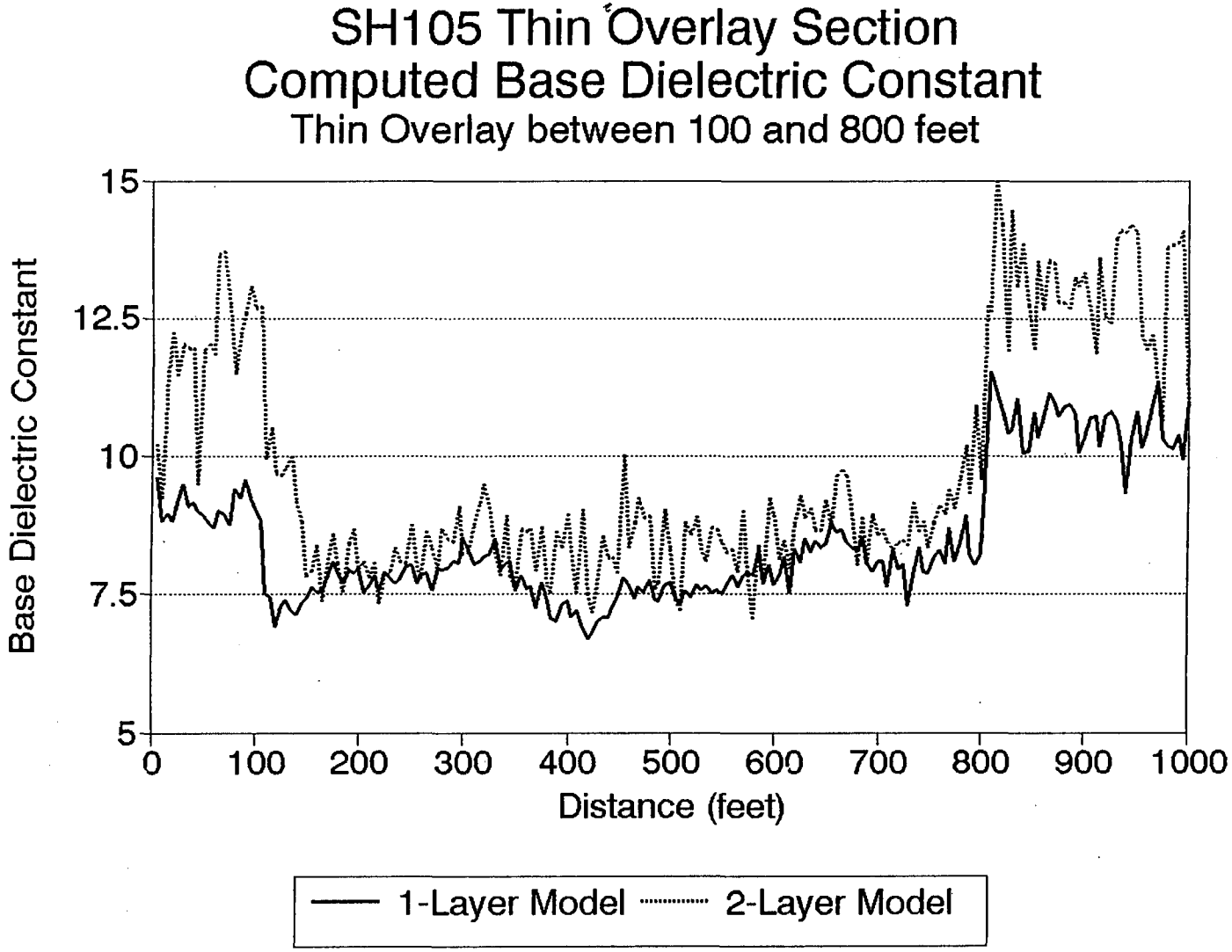

Figure 25. SH 105 Base Dielectric Constant in the Overlay Section.

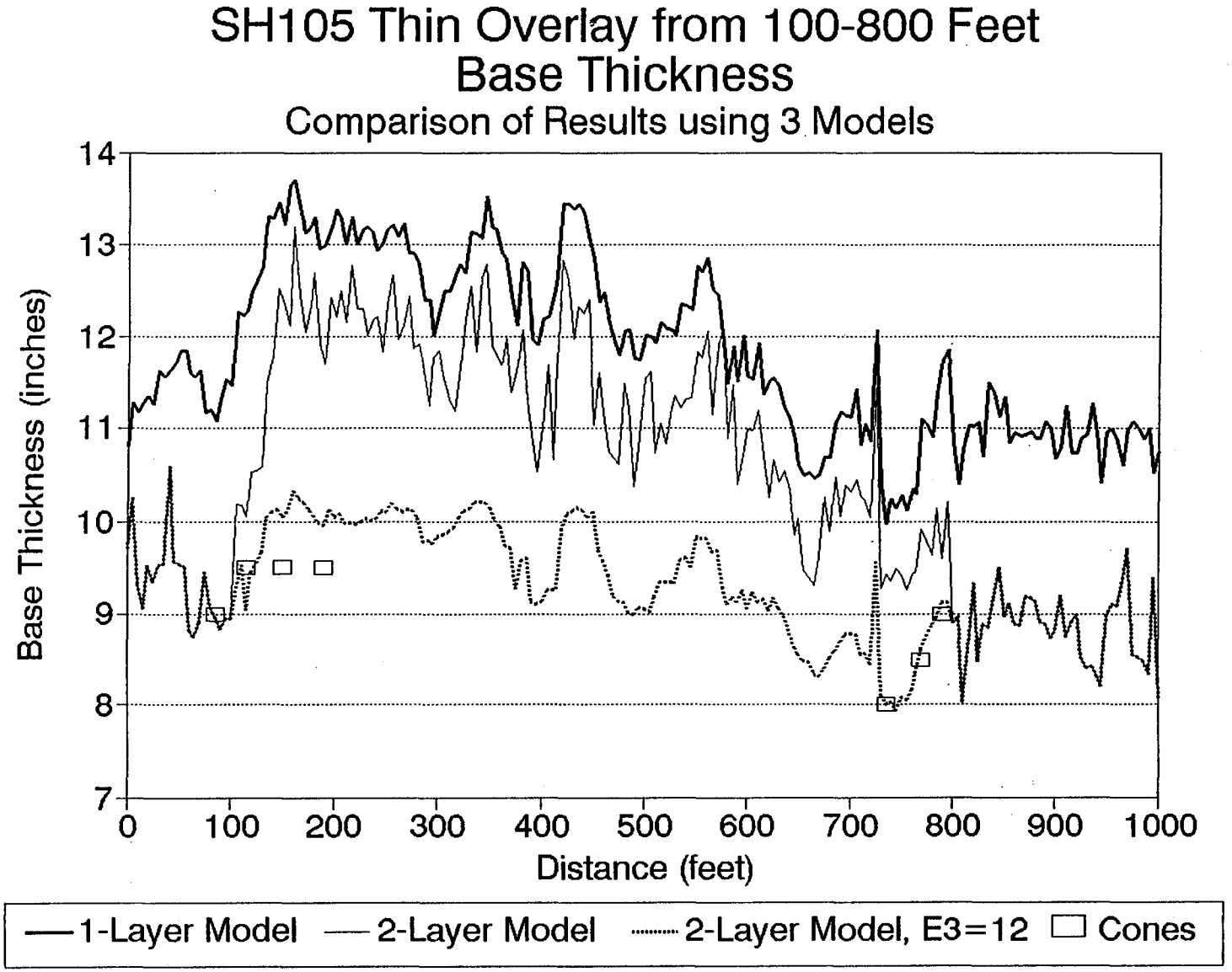

Figure 26. SH 105 Base Thickness in the Overlay Section.

7.2.3 US190 Low Density Overlay

US190 was reported to have a nominal 1" surface course over a 2.5" structural asphalt layer, with a 9" cement stabilized base. The local maintenance personnel indicated that the surface course was composed of expanded lightweight aggregate. The pavement showed numerous transverse cracks, a condition which was attributed to shrinkage cracking of the stabilized base.

Figure 27 shows the surface dielectric constant computed from the radar data. The plot is much more variable that the dielectric plots from sections on SH30 and SH105. The dielectric behavior shows a "background" level of 3.5, with numerous local excursions to a value between 4 and 5. The background level of 3.5 is significantly lower than the typical values of 5 and 6 shown in SH30 and SH105, and in other radar work.

The dielectric constant of 3.5 can be explained by the lightweight aggregate, and supported by calculations using a mixture law. The low value of 3.5 comes because of the much larger percentage of air in the expanded aggregate (dielectric constant = 1) than in normal aggregate. As discussed below, the local deviations from 3.5 do not appear to represent the surface material, but possibly a near-surface condition which is affecting the surface reflection.

For the asphalt thickness calculation, the surface asphalt layer is characterized by the dielectric constant of 3.5, and the resulting asphalt thickness for the two asphalt layers are shown in Figure 28. The results show that the overlay thickness can be calculated separately, and that the total asphalt thickness is slightly underestimated using the two-layer calculation model. This underestimation is due to the low dielectric constant of the first layer, which leads to an interference of the surface reflection by the reflection from the top of the second layer. This interference leads to an overestimation of the second layer dielectric constant, and a corresponding underestimation of the second layer thickness.

A more detailed analysis of the variation in surface dielectric constant is shown in Figure 29, which presents a detailed analysis at 2 foot intervals from 200 to 400 feet. Locations of transverse cracks, determined visually using a survey wheel, are plotted along with the

computed surface dielectric constant. The peaks in the dielectric constant clearly coincide with the locations of the transverse cracks.

Transverse cracking by itself does not explain the anomalous surface reflections that produce these peaks. A more plausible explanation is that moisture entering these cracks migrates laterally into the interface between the two asphalt layers, producing a large reflection. This behavior was also observed in connection with reflection cracking on a Florida section (see Fernando and Maser, 1992). Normally, this large reflection would show up deeper in the data. However, due the thickness low dielectric constant of the overlay, this large reflection subsurface reflection arrives very early. Consequently, it distorts the surface reflection, and produces the apparent peaks in the surface dielectric constant.

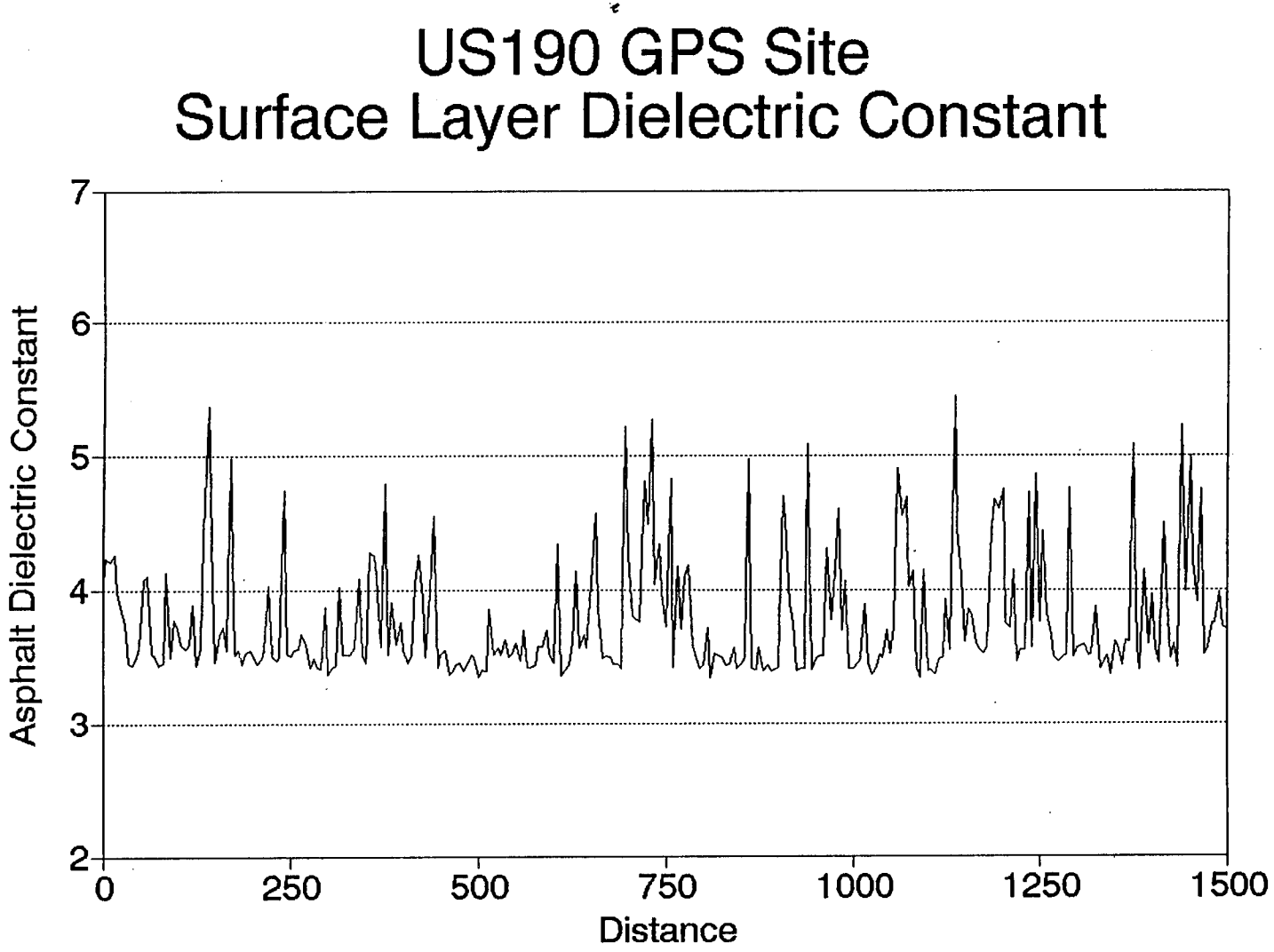

Figure 27. Surface Dielectric Constant on US 190.

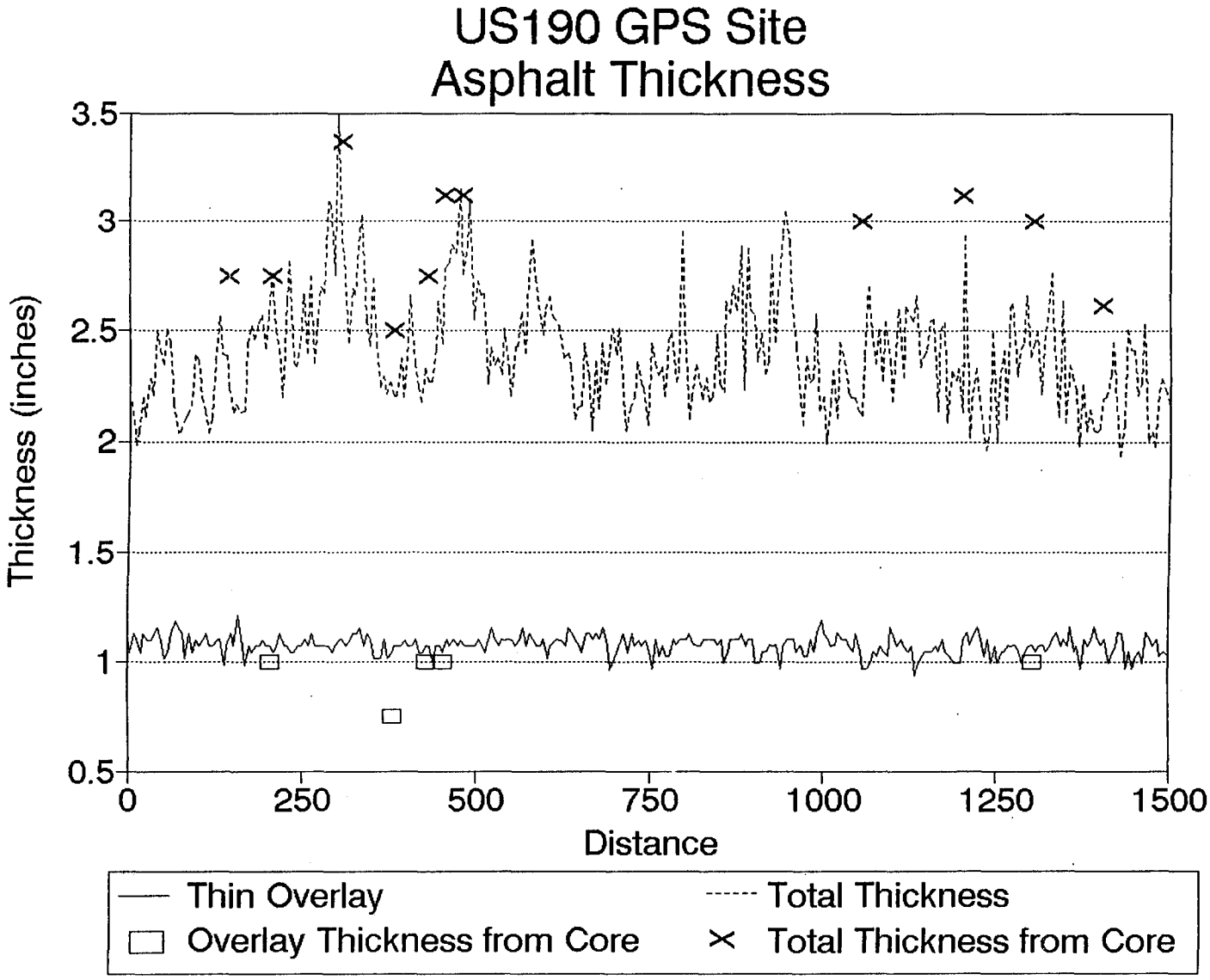

Figure 28. Asphalt Thickness in US 190.

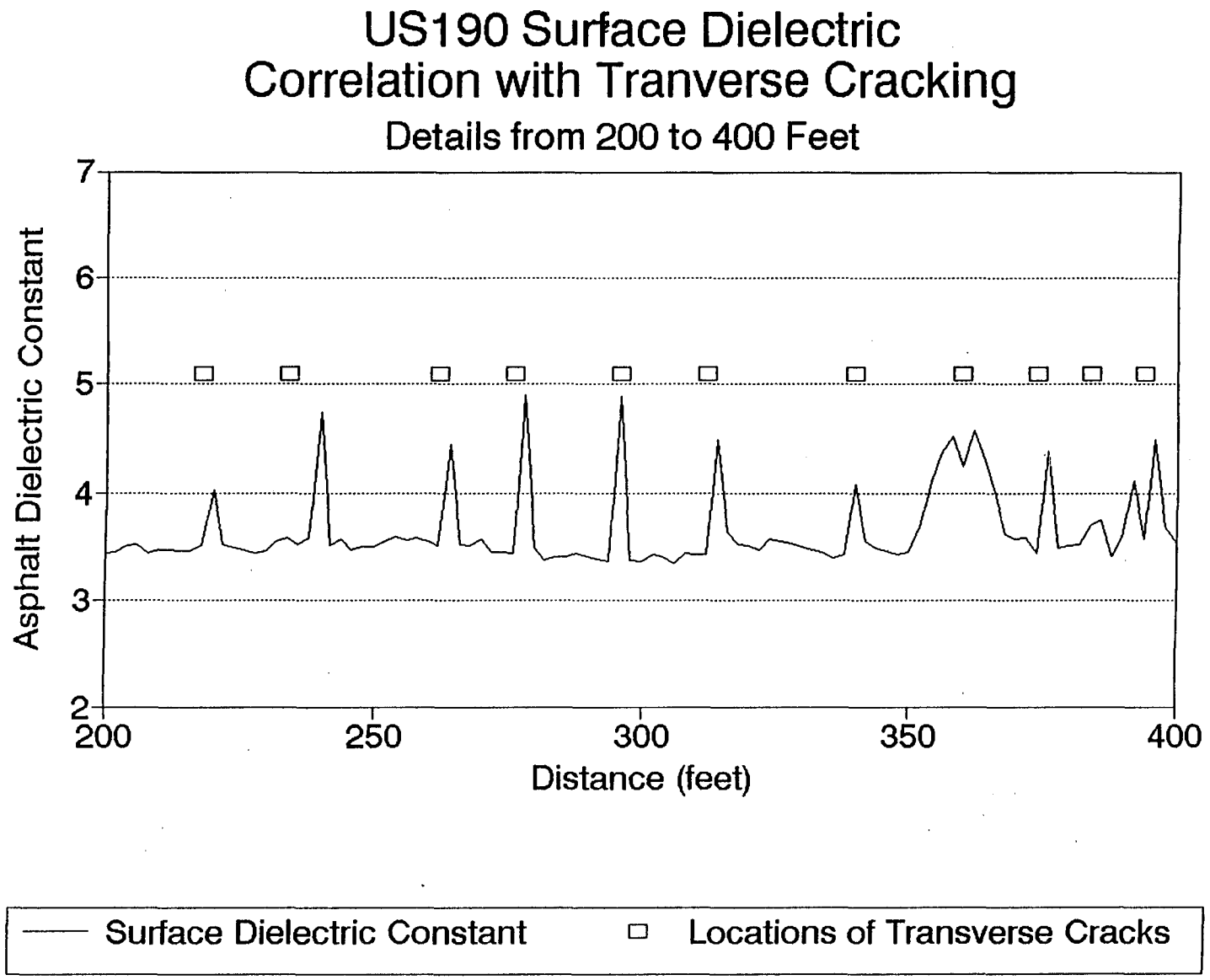

Figure 29. US 190: Correlation of Surface Dielectric with Transverse Cracks.

7.3 Slurry and Chip Seals

Slurry and chip seal sections associated with SPS studies were also placed on SH30 and SH105 sections between the 1990 and 1991 surveys. Similar to the thin overlay, these sections provided an excellent opportunity to focus on the influence of these surface treatments on the radar data. Slurry and chip seal sections on both SH30 and SH105 had 100 foot transition sections at each end, allowing for core sampling and thickness correlations.

The slurry and chip seal sections were analyzed in two alternative ways: (a) ignoring the surface treatment; and (b) treating the surface treatment as a distinct layer. An example of the latter analysis is shown in Figure 30, where waveforms from the chip seal section of SH30 have been processed with the surface reflection removed. The removal of the surface reflection produces a residual which does not have the shape of a true layer reflection like that seen in the thin overlay. This residual represents the distortion of the surface reflection caused by the overlay. The (b) analysis treats this reflection as if it represents a distinct layer.

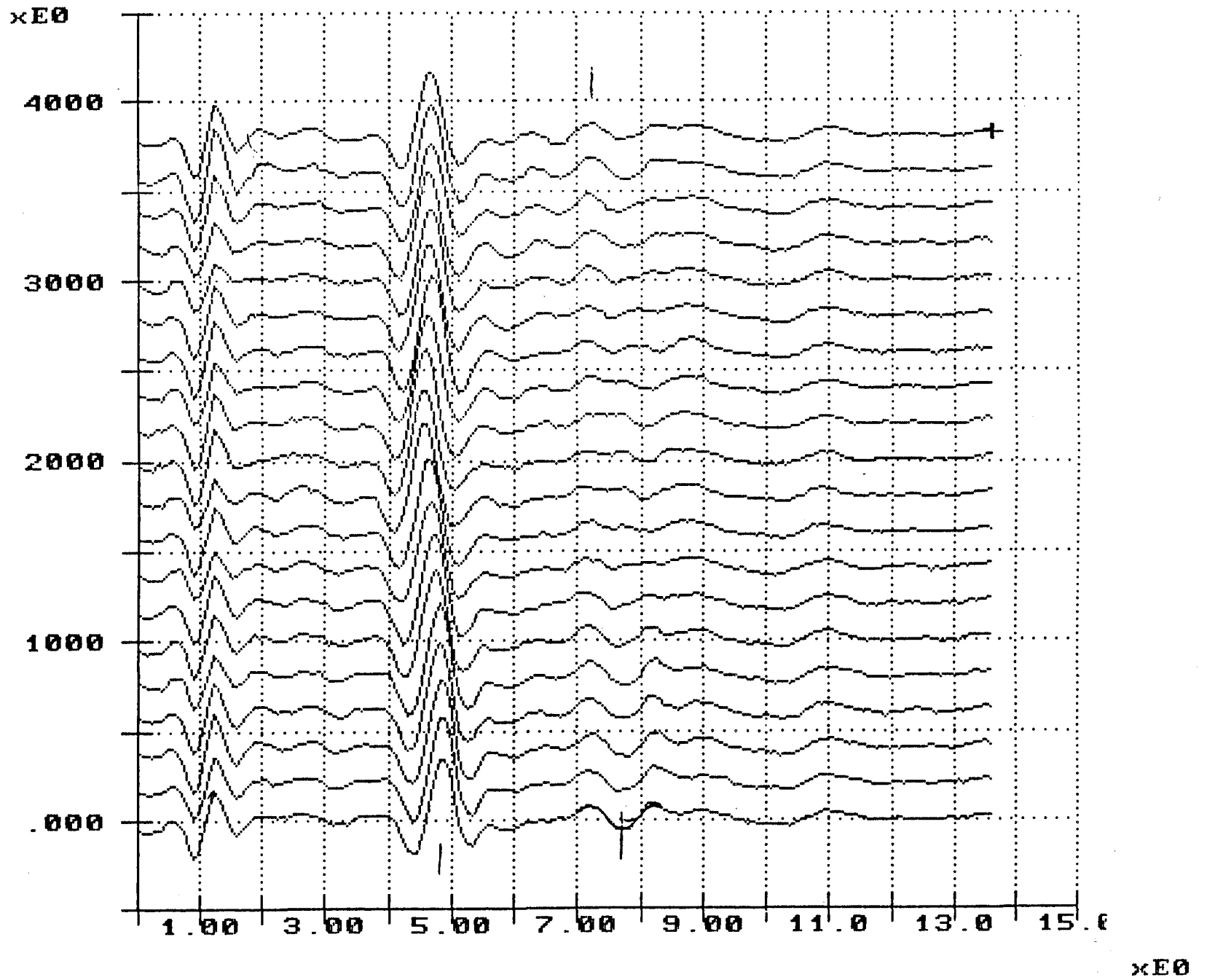

Figure 30. SH 30 Waveforms Showing Effect of Slurry Seal.

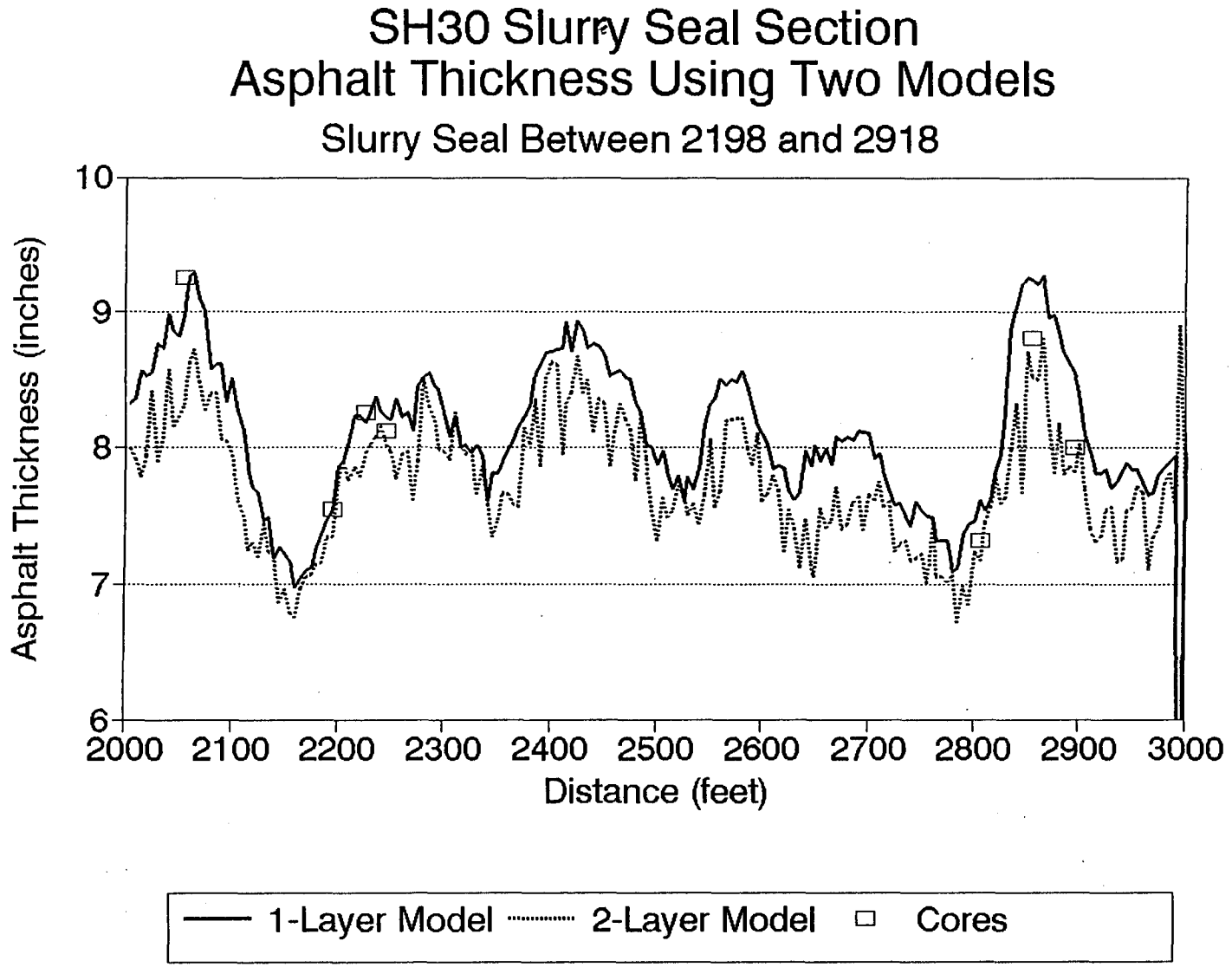

Figure 31. SH 30 Asphalt Thickness in the Slurry Seal Section.

7.3.1 Slurry Seal on SH30

Figure 31 shows two asphalt thickness analyses, one in which the asphalt is treated as a single layer with the residual ignored, and one in which the residual is treated as a reflection from an intermediate layer. The results show little difference between the two analyses, and the correlation with the core values appears to be good.

A more significant difference shows up in the calculation of base thickness. Figure 32 shows the calculation of base thickness using the two models described above. Apparently, a model which ignores the surface treatment produces better results for these base thickness predictions. Note from Figure 33 that the subgrade reflection amplitude varies considerably at the core correlation locations, and that the poor correlation at location 2050 feet might be due to the detection of the wrong peak.

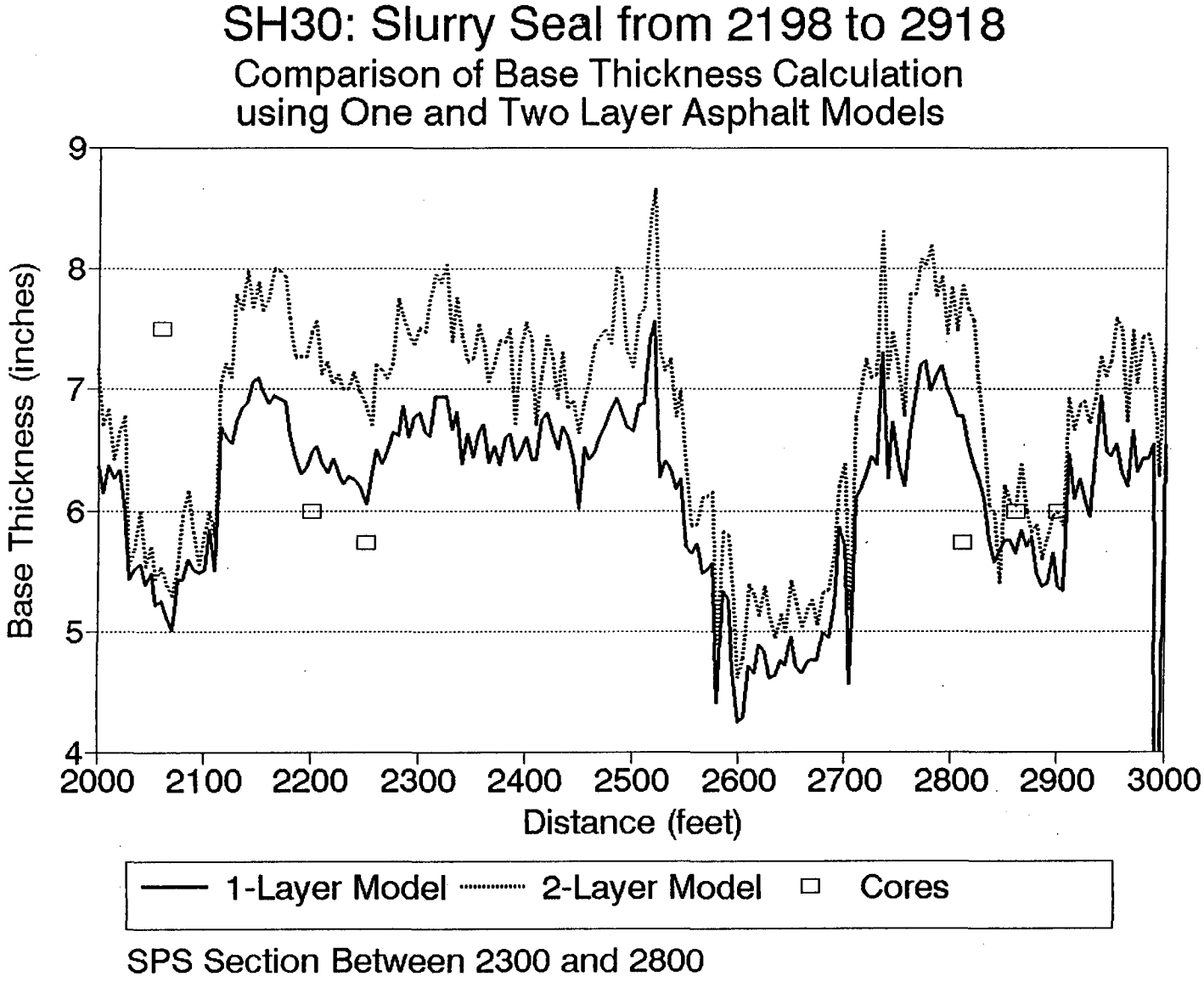

Figure 32. SH 30 Base Thickness in the Slurry Seal Section.

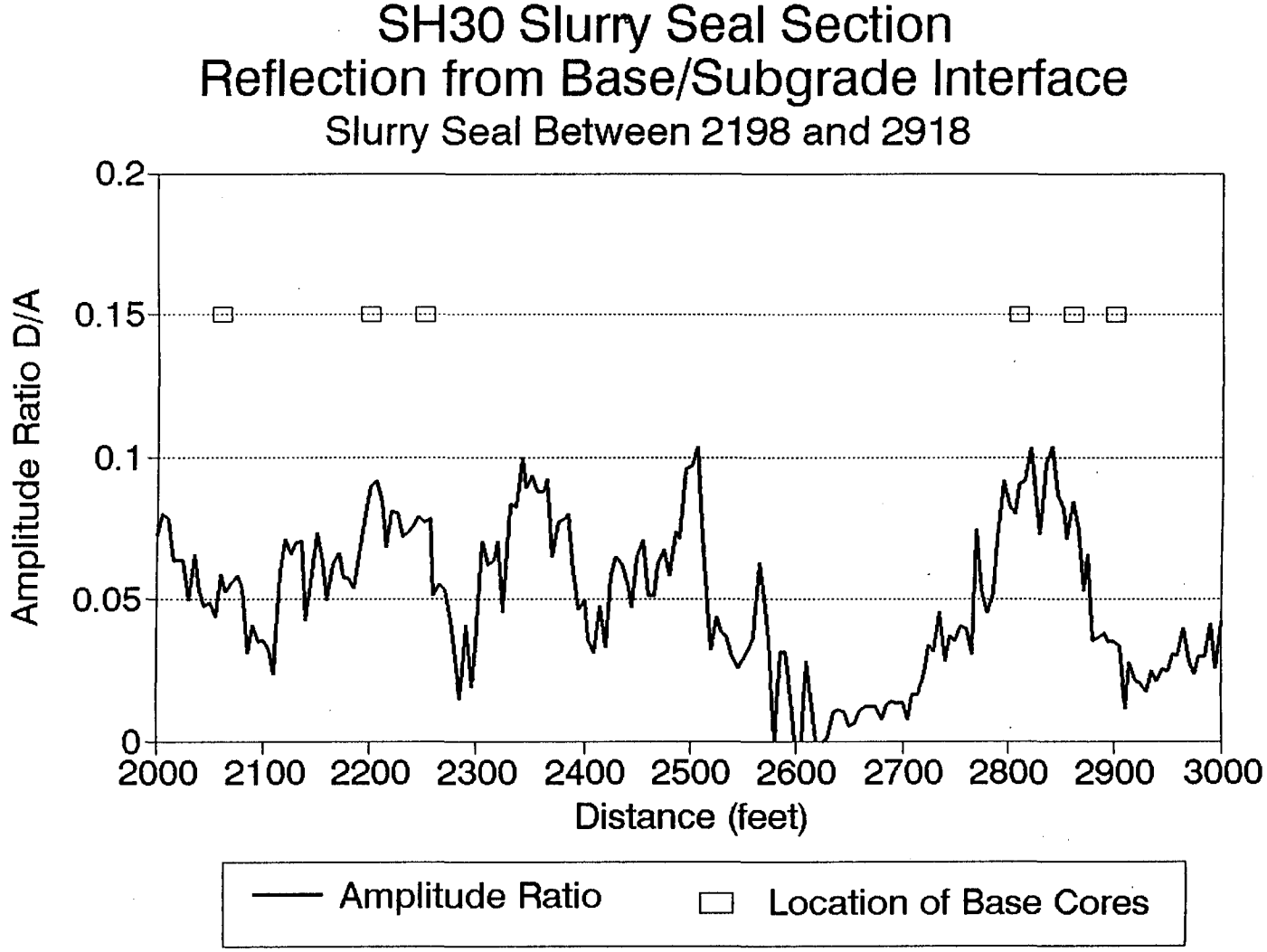

Figure 33. SH 30 Normalized Base/Subgrade Reflection in Slurry Seal Section.

7.3.2 Chip Seal on SH30

Figure 34 shows the asphalt thickness results for the one- and two-layer models for the SH30 chip seal section. The core data lies in between the results from these two models, but seems to favor the one-layer model. Figure 35 shows the base thickness calculations using the two models. Note that some base thickness calculations are very close to the core values (at 300, 400, and 1050 feet), while other are very different from the cores. An examination of the base/subgrade reflection amplitude in Figure 36 shows a large percentage of this data below 0.05, which suggests the possibility that the base has been mistracked. The base data for the highest base/subgrade reflection (at 300 feet) is the most accurate. Given these observation, it appears that better representation of the base thickness is obtained by ignoring the chip seal.

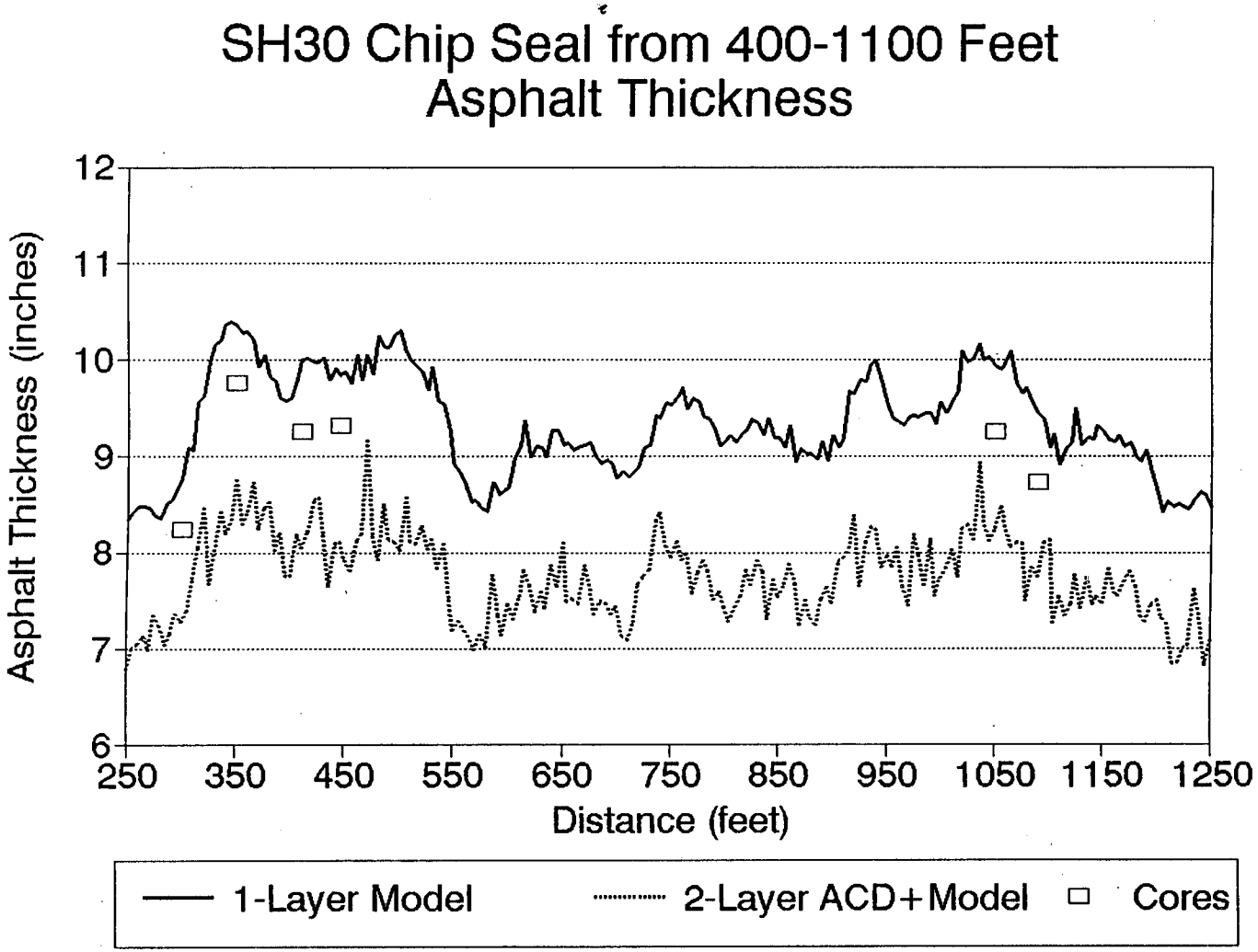

Figure 34. SH 30 Asphalt Thickness in the Chip Seal Section.

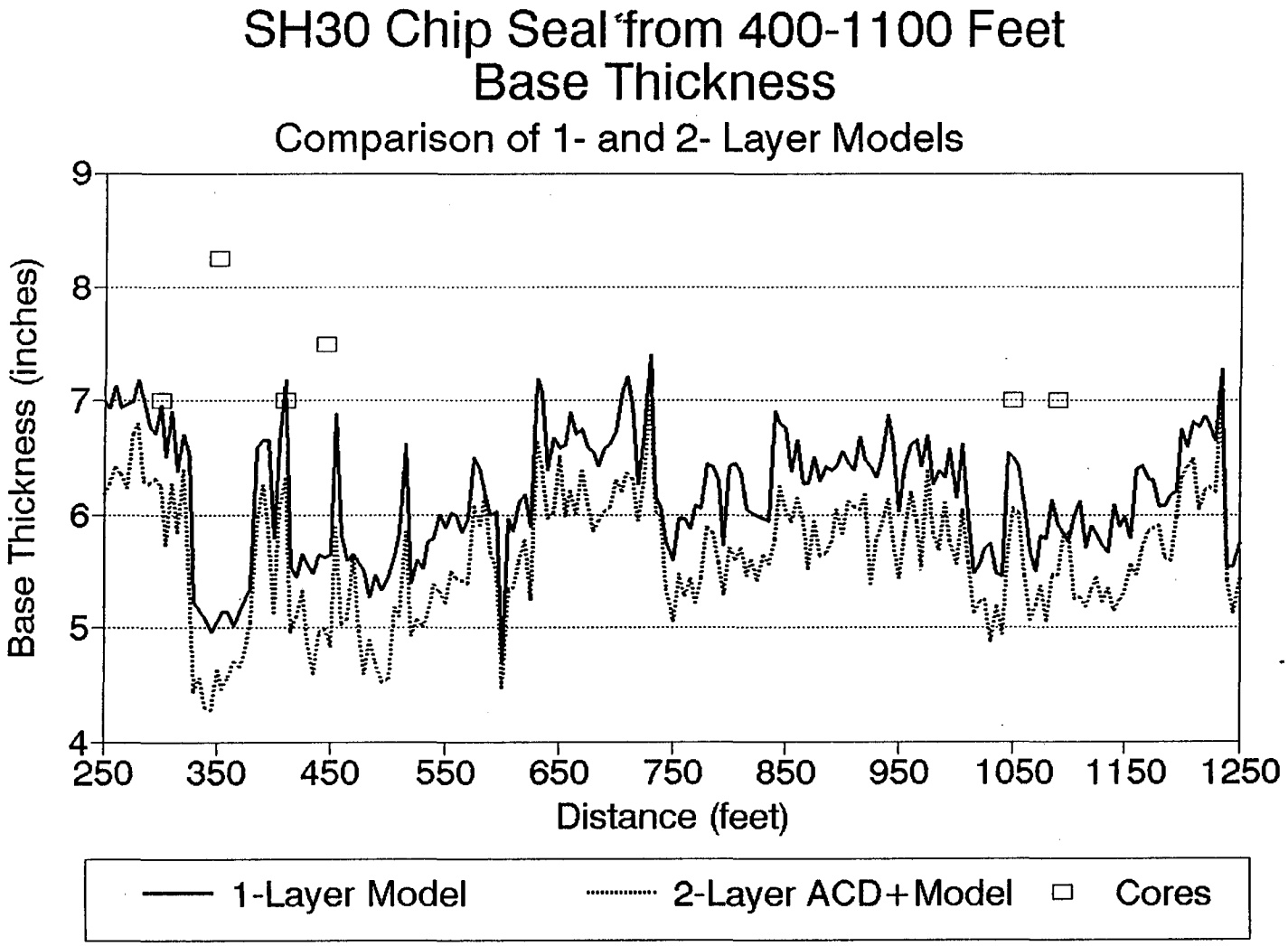

Figure 35. SH 30 Base Thickness in the Chip Seal Section.

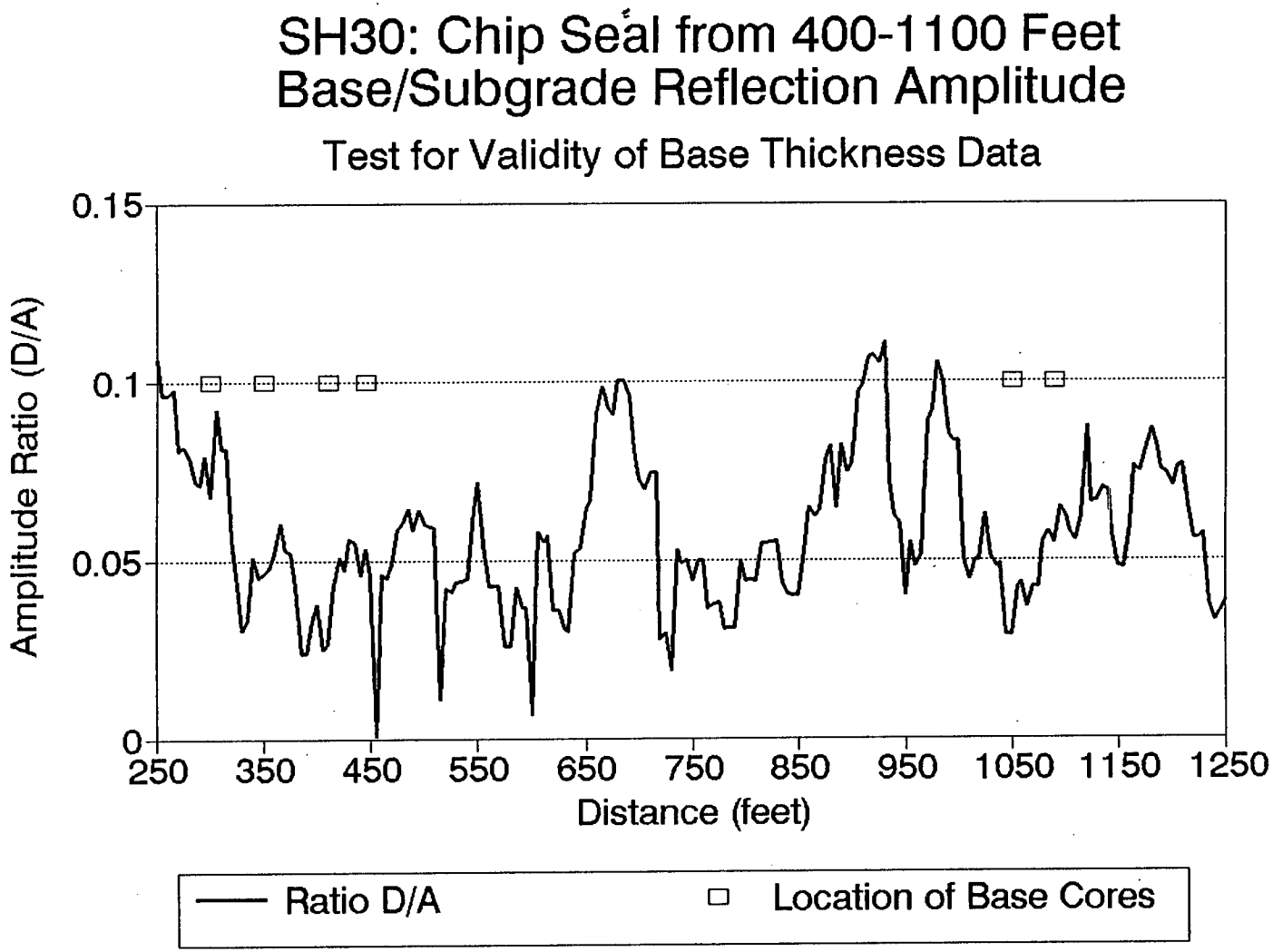

Figure 36. SH 30 Normalized Base/Subgrade Reflection in Chip Seal Section.

7.3.3 Slurry Seal on SH105

Figure 37 shows the asphalt thickness calculations for the slurry seal section of SH105. The figure also shows the calculation of the thickness of the first layer of the two-layer model, and compares that calculation to the core measurements of this first layer. Note that the one-and two-layer models presented here are the same as those used earlier in the GPS site, with no special consideration for the slurry seal. The results show that the one-and two-layer models produce similar thickness results, and the two layer model is more accurate. The results also show that the calculation of the first asphalt layer closely matches the core measurements.

Figure 38 shows the base thickness calculations with the one-and two-layer models. The superiority of the two layer model for this site is clearly evident in the computation of the base thickness. Figure 39, showing the base/subgrade reflection amplitude, indicates that the reflection is strong in the areas where the cores were taken. One would expect more accurate base thicknesses under these circumstances than under the SH30 conditions, where the reflection was weak.

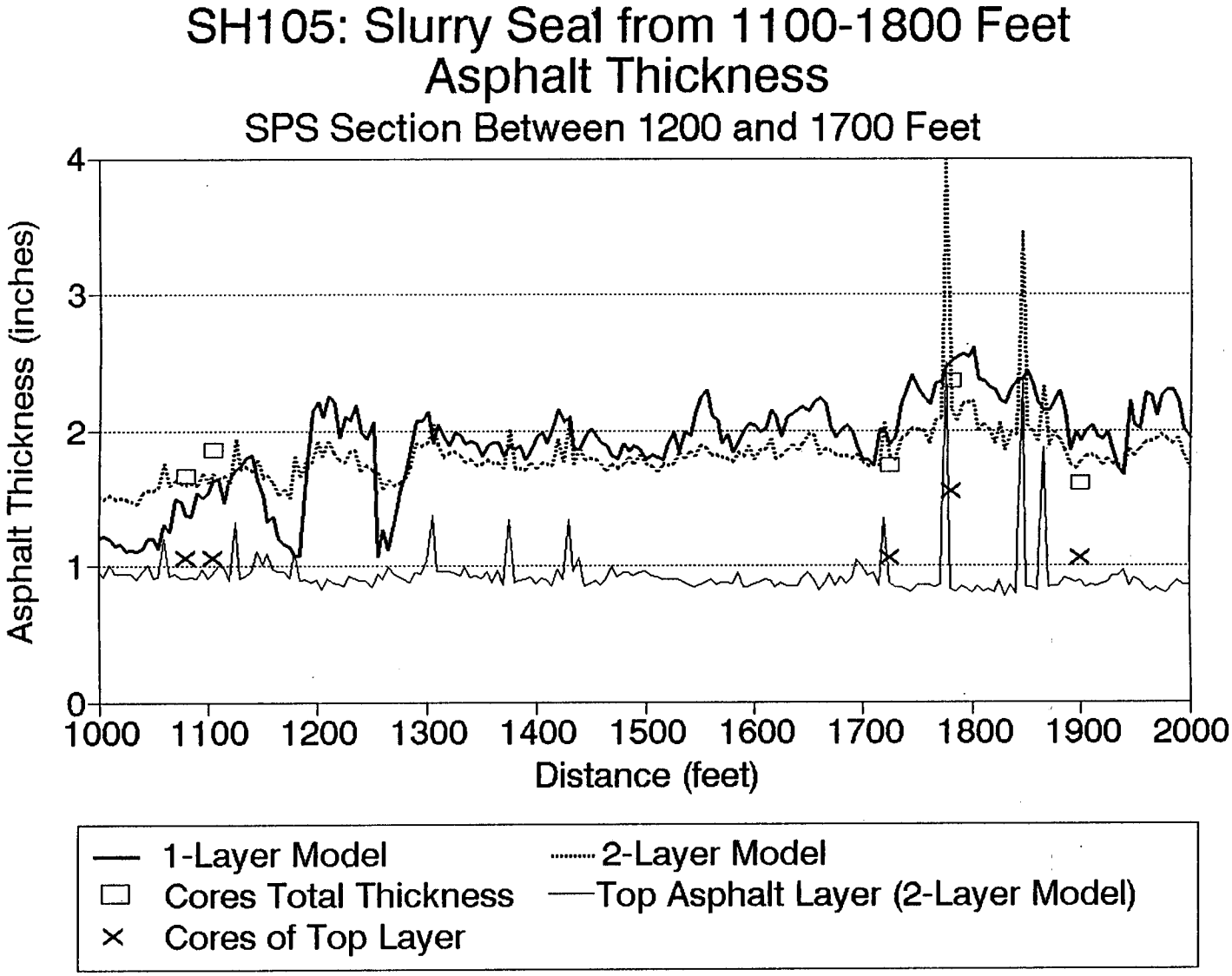

Figure 37. SH 105 Asphalt Thickness in the Slurry Seal Section.

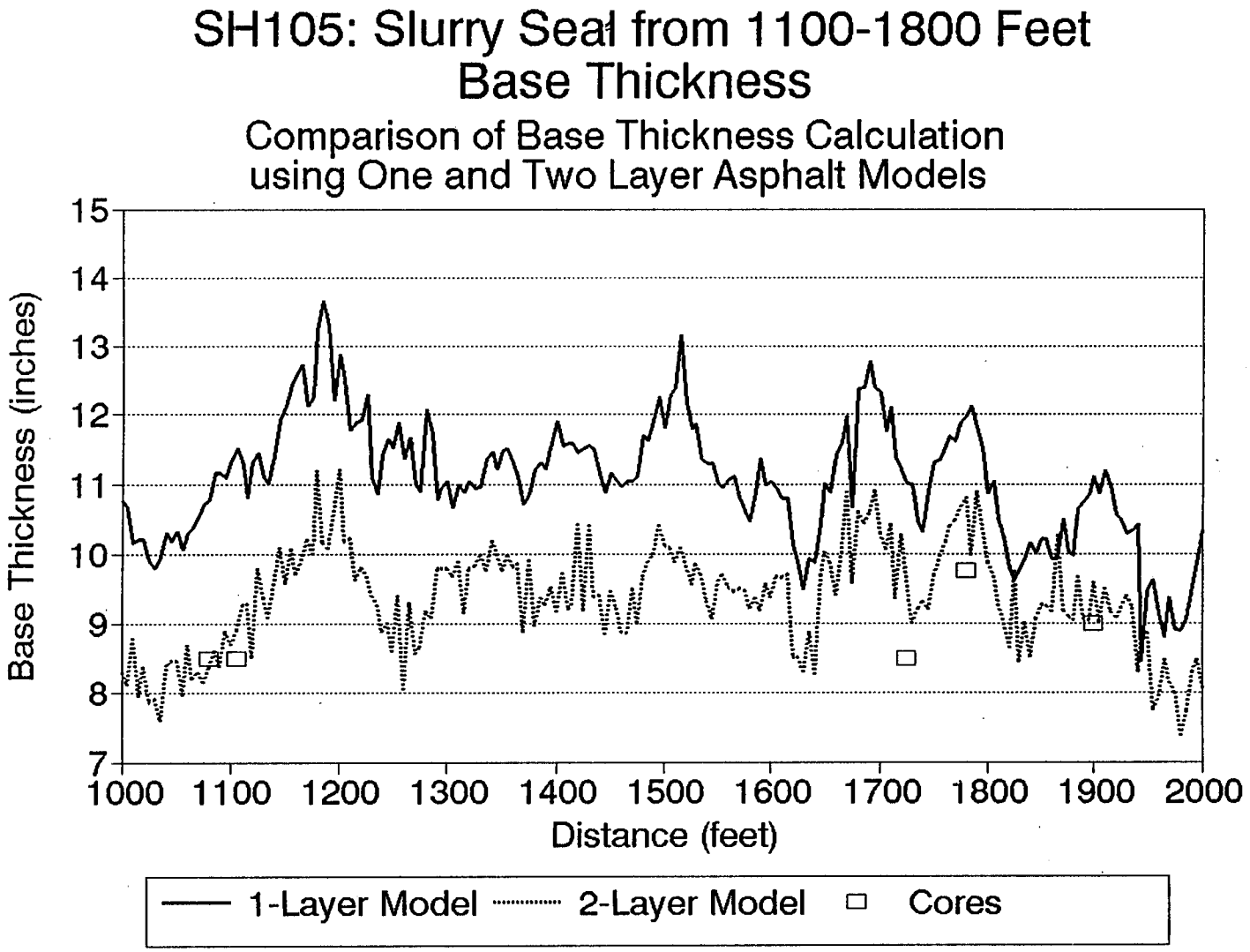

Figure 38. SH 105 Base Thickness in the Slurry Seal Section.

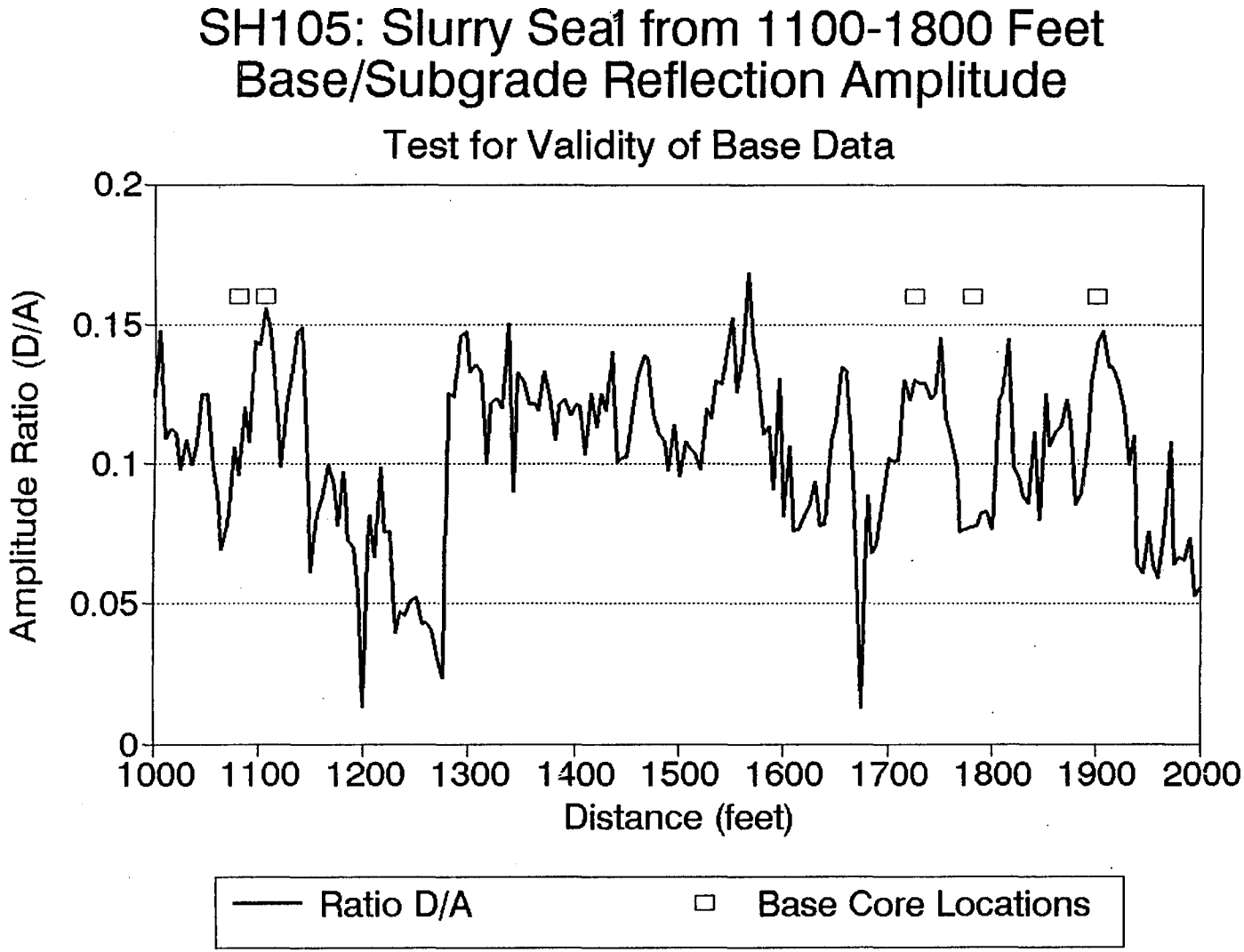

Figure 39. SH 105 Normalized Base/Subgrade Reflection in Slurry Seal Section.

7.3.4 Chip Seal on SH105

Figure 40 shows the asphalt thickness results for the chip seal section of SH105. The two-layer model results show a strong correlation between cores and calculations for both the total asphalt thickness and the top asphalt layer. Figure 41 shows the base thickness calculations for both the one- and two-layer model. These results again show that it is necessary to model the asphalt as two layers in order to obtain accurate base thickness results, and that no special consideration is required for the chip seal. The base/subgrade reflection amplitude, shown in Figure 42, indicates a strong and clear interface.

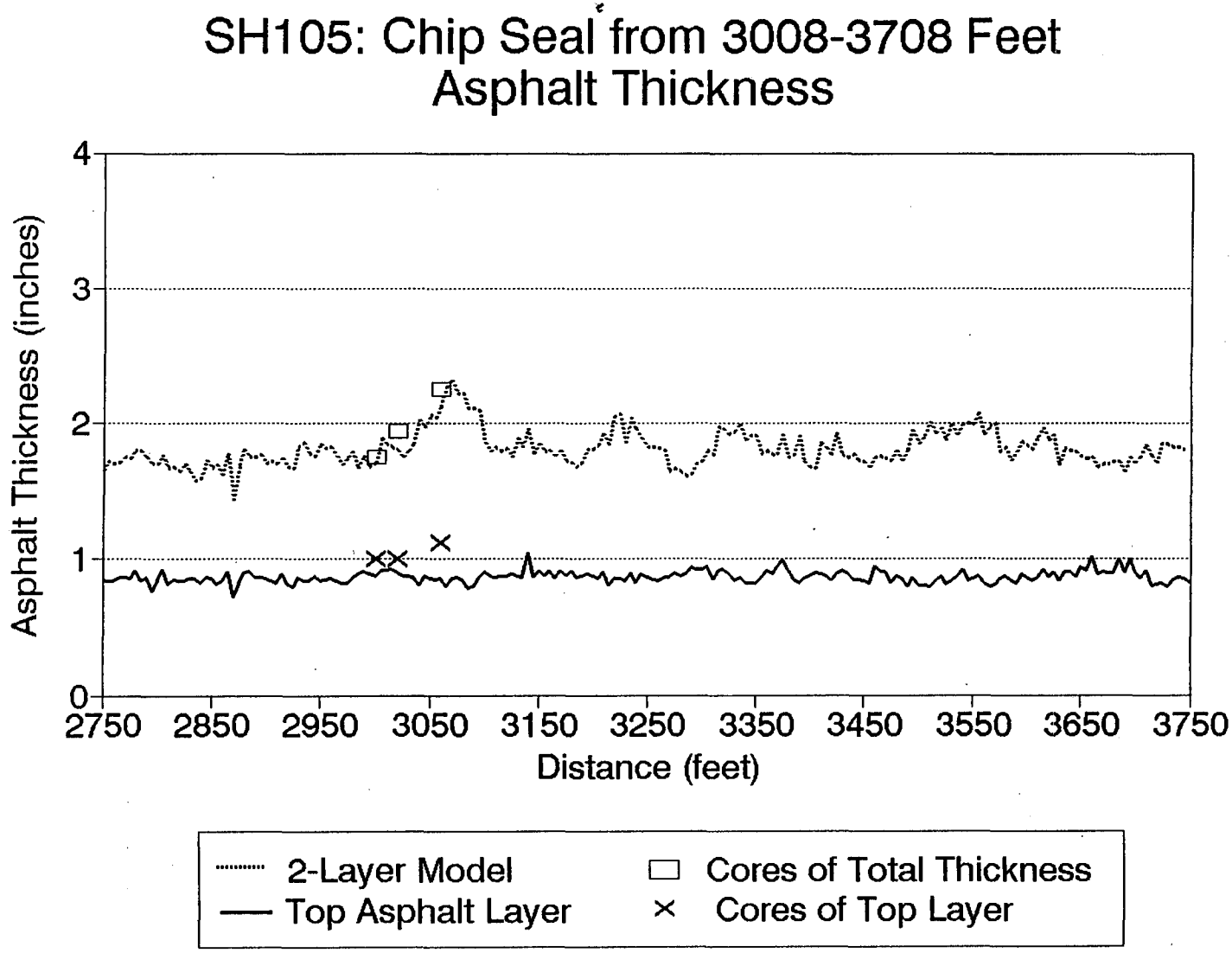

Figure 40. SH 105 Asphalt Thickness in the Chip Seal Section.

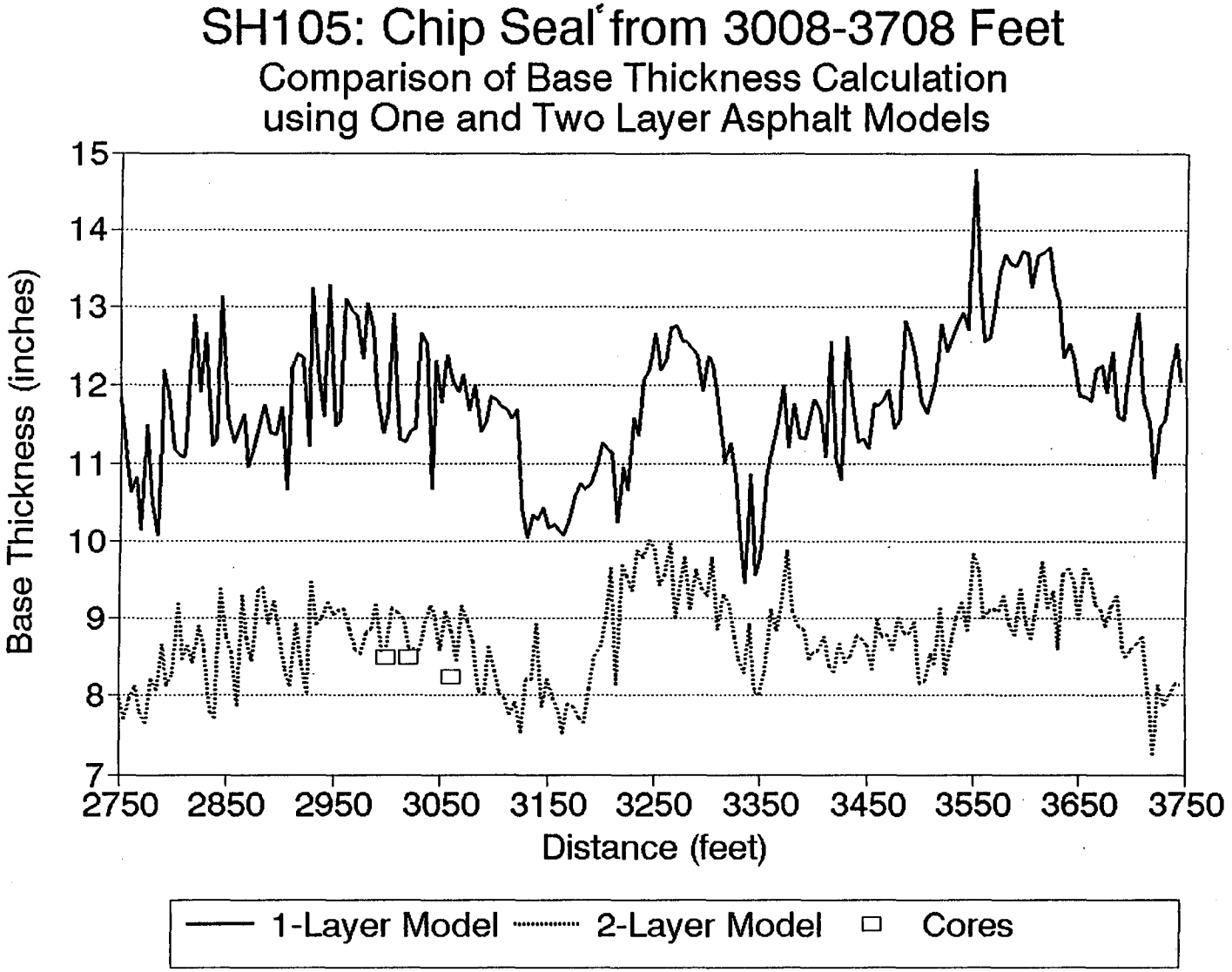

Figure 41. SH 105 Base Thickness in the Chip Seal Section.

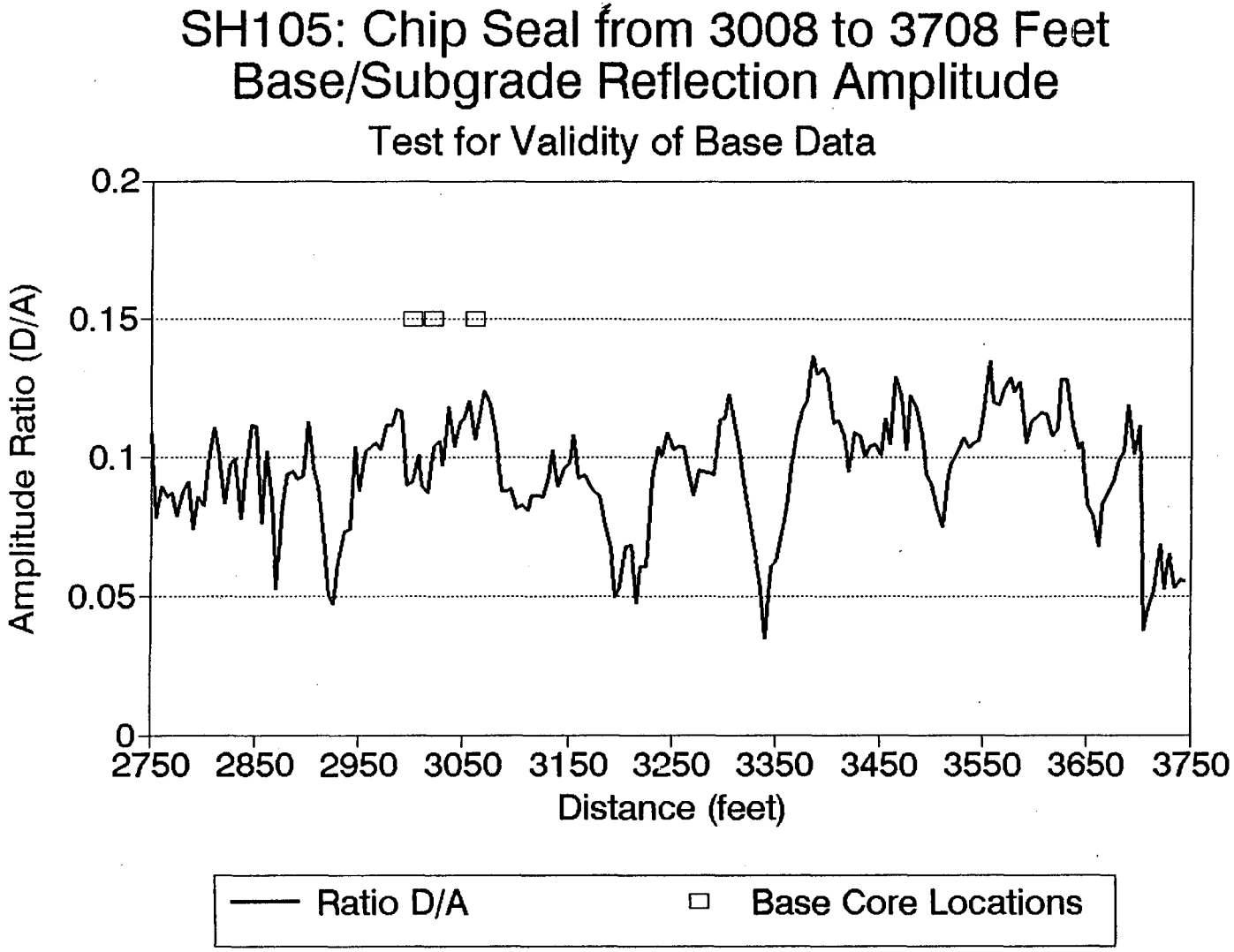

Figure 42. SH 105 Normalized Base/Subgrade Reflection in Chip Seal Section.

7.4 Correlations Between Radar and Cores

A tabulation of radar thickness calculations vs. core measurements for all core sites is presented in the Appendix of this report. Table 1 summarizes the rms deviations between radar and core values by pavement section, by site, and for the entire study.

Table 1. Summary of Radar Accuracy

Site	Equipment	RMS Deviation (inches) Asphalt	Base	
			As Computed	With D/A > 0.06
SH30 GPS	R-II	0.31	1.0	0.47
	PS-24	0.19	2.3	0.77
SH105 GPS	R-II	0.47	1.29	1.29
	PS-24	0.17	1.07	1.11
US190 GPS	PS-24	0.56	--	--
SH30 Chip Seal	PS-24	0.64	1.60	0.03
SH30 Slurry Seal	PS-24	0.27	1.07	0.61
SH105 Chip Seal	PS-24	0.11	0.34	0.34
SH105 Slurry Seal	PS-24	0.15	0.76	0.76
SH105 Overlay	PS-24	0.20	0.33	0.33
SH30 All Sites	PS-24	0.35	1.00	0.77
SH 105 All Sites	PS-24	0.17	0.81	0.81
All Sites	PS-24	0.33	1.00	0.77

The table shows overall accuracies for asphalt thickness that are comparable to those of previous studies. Locally, higher accuracies were achieved at most sites. However, the condition at US190 and the chip seal at SH30 produce lower accuracy which adversely affect the overall average. The deviation for SH105 (0.17 inches) is half of that for SH30 sites (0.35 inches). On a percentage basis, however, with SH105 nominally 2.25 inches thick and SH30 nominally 8" thick, the accuracy is 7.5% for SH105 and 4.3% for SH30.

The table also shows that the use of a threshold base/subgrade reflection value prior to base thickness computation increases the accuracy of the base thickness data. This is especially important when the base/subgrade reflection is weak (i.e., SH30). Finally, the table

reveals differences between the R-II and PS-24 radar systems. The R-II system, as discussed earlier, appears to produce better resolution of base thickness when the base/subgrade interface is weak. The PS-24, on the other hand, appears to produce more accurate thickness values for the surface layers.

Figures 43 and 44 show summaries of the overall correlation between cores and radar thickness measurements. The regression statistics for the asphalt thickness are similar to those obtained in previous studies. The statistics for the base thickness are improved, in that there is a slope of close to 1.0, and an intercept close to 0. The R-square is similar to that shown previously (Maser and Scullion, 1991), but it appears to be due mainly to a few outliers. These outliers should be reviewed in further detail to see if (a) the peak was mistracked, or (b) the ground truth data is potentially flawed. It was noted by Maser and Scullion that the use of penetrometer and visual data for base ground truth had the potential for error.

Summary of Radar vs. Cores Asphalt Thickness

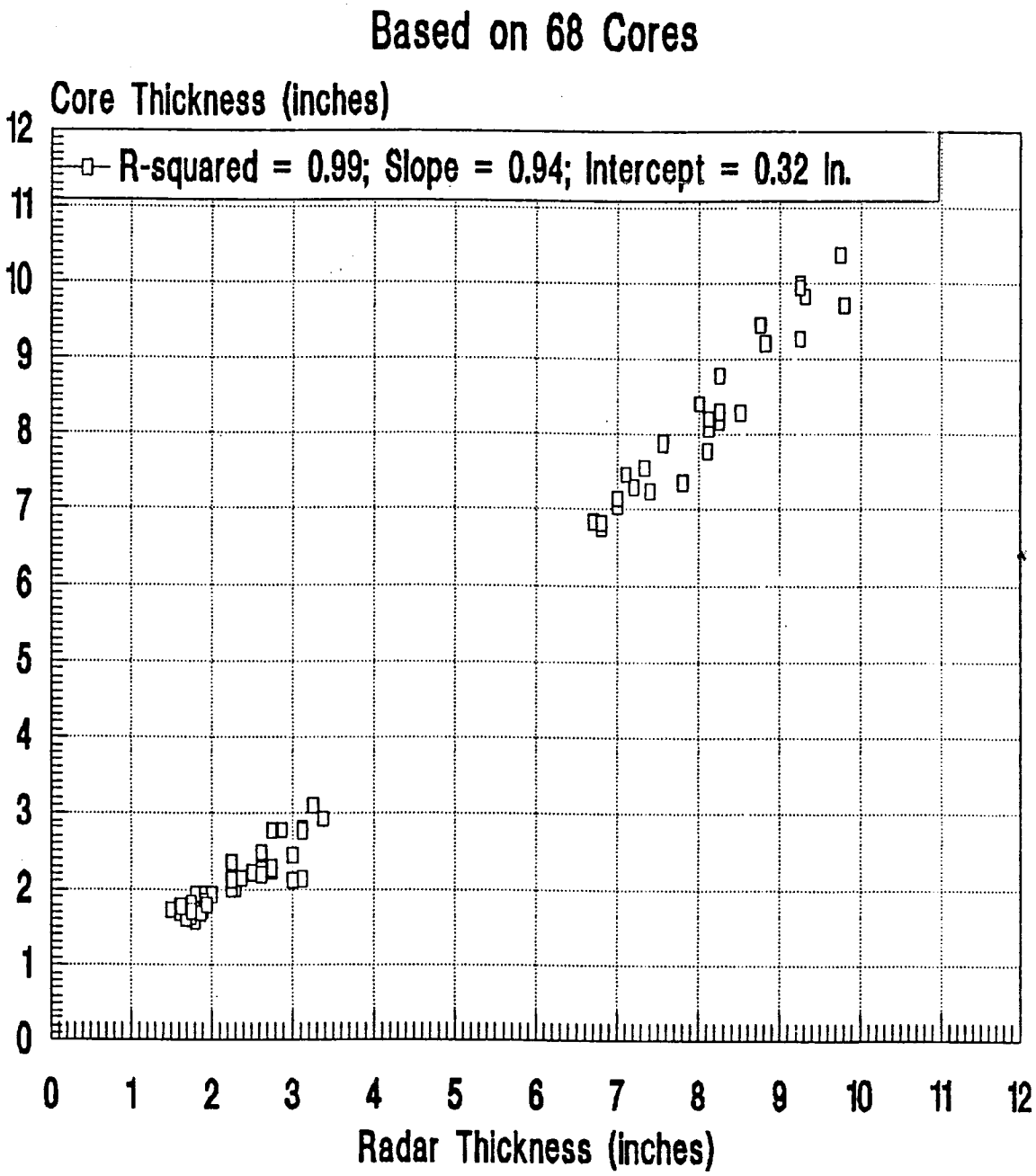

Figure 43. Cores vs. Radar for Asphalt Thickness.

Summary of Radar vs. Cores
Base Thickness

Based on 40 Cores

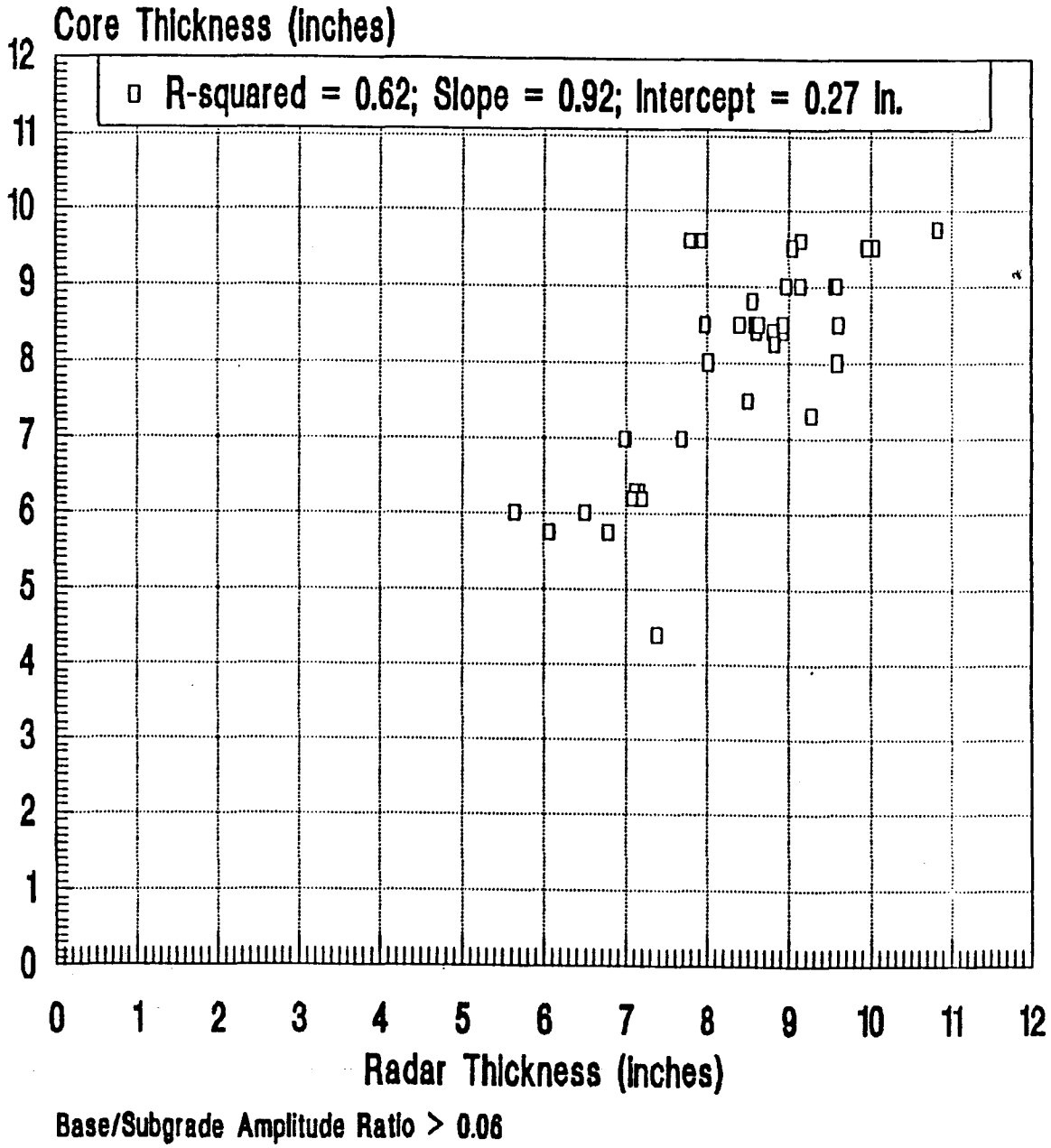

Figure 44. Cores vs. Radar for Base Thickness.

CHAPTER 8
DISCUSSION

8.1 Comparison of Penetradar PS-24 and Pulse Radar R-II Equipment

The results in section 7.1 and 7.4 show that the reflection from the base/subgrade interface is significantly weaker for the PS-24 system for both the SH30 and the SH105 sites. The results also show that for the thin asphalt layers on SH105, the PS-24 produces more accurate asphalt thickness data. These two observations suggest that the PS-24 has a higher frequency content, giving it better resolution at close range but more attenuation for deeper layers.

This suggestion could be tested by observation of the magnitude of the FFT of the plate reflections for each of these two antennas. In such a comparison, each antenna would have to be placed at the same height over a plate of the same size. Such comparative data is not currently available.

Two additional observations are worth noting. Figure 45 shows that the PS-24 has signal distortion in the range where the base reflection amplitude appears for the two sites tested. This noise, which appears in the metal plate reflection, is possibly due to multiple antenna reflections or to reflections from the van. This noise may be interfering with the base/subgrade reflection for the particular sites which were evaluated. The R-II has similar noise, but it occurs much later in the signal.

8.2 Thin Overlays

The results in Sections 7.1.2 and 7.2 show that the thickness of thin overlays of approximately 1 inch can be accurately calculated with the 1 GHz equipment used in this study. The thickness of the existing overlays on SH105 and US190 was accurately evaluated, as well as the thickness of the new overlays placed as part of the SHRP SPS study. The ability to detect such layers depends on the existence of a dielectric contrast between the overlay and the existing material. In SH105, the iron ore aggregate in the first overlay appeared to provide such a contrast. In addition, new asphalt usually will differ from the existing asphalt

because of the aging of the latter. These results suggest that radar can be used for quality control of newly placed overlays.

The results of Sections 7.1.2 and 7.2 also show that accounting for such overlays in the analysis greatly improves the accuracy of the base thickness computation. The need to take the overlay into account depends on whether it produces a dielectric contrast which must be considered in the layer model. Future work should seek to develop simple algorithms for detecting the presence of a thin overlay without requiring detailed processing. A number of possible algorithms exist, but they would have to be implemented and tested on a larger data set.

The results for US190 show, however, that when the travel time in the overlay is too short (due either to thicknesses < 1 inch and/or dielectric constants < 5), interference with the surface reflection will occur, leading to reduced accuracy of thickness calculations.

8.3 Slurry and Chip Seals

The results presented in Section 8.3 show that the presence of slurry and chip seals had little effect on the asphalt and base thickness predictions. Attempts to model these seals as distinct layers tended to produce errors between radar analysis and cores, for both asphalt and base thickness.

8.4 Moisture in the Asphalt Layers

The anomalous near surface reflections seen on the SH30 thin overlay and on US190 appear to be related to moisture trapped under the overlay. However, no data confirming the presence of interlayer moisture at these locations has been collected. When this type of behavior occurs, more accurate results are obtained when the "background" dielectric constant of the second layer is used in the analysis.

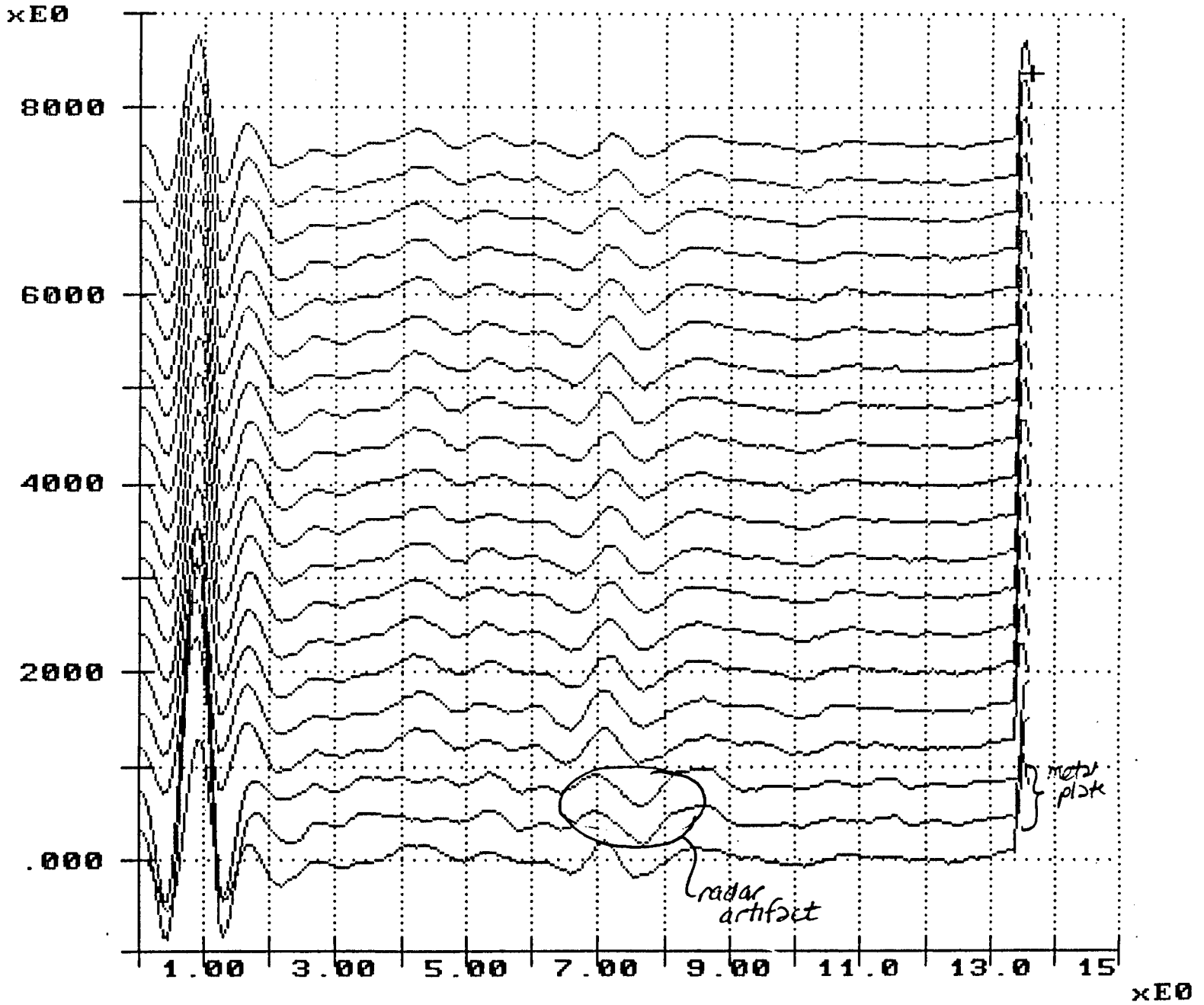

Figure 45. Metal Plate Reflection Using the PS-24 Antenna.

CHAPTER 9
CONCLUSIONS

The results of this study have illustrated the influence of overlays and surface treatments on the accuracy of pavement thickness calculations using radar.

Thin Overlays

Where there is a significant contrast between the overlay and the existing pavment, it is (a) possible to accurately measure the overlay thickness for thickness as low as 1 inch; and (b) necessary to account for the overlay in order to obtain accurate thickness values for the deeper layers.

Slurry and Chip Seals

It appears that these can be ignored in the thickness computation. For chip seals, the results may be slightly less accurate due to the distortion which it creates on the surface reflection.

Overall Accuracy

The results of this study have confirmed previously reported accuracy levels for asphalt thickness evaluation (+/- 0.33 inches; or +/- 5% to 7.5%). They have also shown potential improvement in base thickness calculations (+/- 0.77 inches; or +/- 9.5%) by using the base/subgrade reflection test and by considering the overlay in the thickness model.

Moisture Between Asphalt Layers

There is strong evidence that this can be clearly detected in the radar data. However, it is necessary to confirm this evidence with controlled field sampling and laboratory moisture tests.

Differences in Radar Equipment

There are subtle differences between otherwise comparable 1 GHz horn antenna radar systems. These differences could be more clearly quantified with tests to isolate system clutter, and frequency domain evaluation of the system output.

REFERENCES

Chung, T. and Carter C. R. "Radar Signal Enhancement for DART," Report MAT-89-05 published by Research and Development Branch, Ontario Ministry of Transportation, Downsview, Ontario, CANADA. June 1989.

Halabe, U.B., Maser, K., and Kausel, E. "Condition Assessment of Reinforced Concrete using Electromagnetic Waves," Final Technical Report prepared for the U.S. Army Research Office under Contract DAAL 03-87-K005, Center for Construction Research and Education, Massachusetts Institute of Technology, Cambridge, Massachusetts. 1989.

Maser, K.R. and Scullion, T. "Automated Pavement Subsurface Profiling Using Radar- Case Studies of Four Experimental Field Sites," TRB Preprint No. 91-0796. January 1991.

Maser, K.R., "Automated Detection of Pavement Layer Thickness and Subsurface Moisture using Ground Penetrating Radar," Report submitted to the Texas Transportation Institute and the Texas State Dept of Highways and Public Transportation. November 1990.

Maser, Kenneth R. "Radar Pavement Thickness Evaluations for Varying Base Conditions: Case Studies at 14 Kansas Sites," Report Prepared for the University of Kansas, Department of Civil Engineering. December 1991.

Roddis, W. M. Kim, Maser, Kenneth R., and Gisi, Andrew J. "Radar Pavement Thickness Evaluations for Varying Base Conditions," TRB Preprint No. 920682. January 1992.

APPENDIX - Summary of Radar vs. Cores

Distance	Asphalt Core	Pulse 1 Asphalt	Penet Asphalt	Base Core	Pulse 1 Base	Penet Base	Pulse R3	Penet R3
SH30 GPS								
212	7.8	7.775059	7.35	6.7	6.582095	6.410712	.054	.03
252	801	7.803653	7.78	6.6	7.045050	5.624536	.059	.034
392	8.12	7.679234	8.07	7	6.472389	6.985557	.09	.086
447	6.7	6.715219	6.844624	6.3	6.516627	7.155037	.069	.142
452	6.7	6.803959	6.823602	6.3	6.758624	7.101594	.054	.127
457	6.8	6.729555	6.762680	6.2	6.577856	7.068050	.068	.104
462	6.8	6.839495	6.821840	6.2	6.617766	7.195794	.053	.104
1039	7	6.911864	7.04	6.5	6.840026	10.18757	.054	.031
1064	7	7.108202	7.14	6.5	7.279941	9.689799	.056	.031
1069	7.2	7.874130	7.288774	5.8	8.386515	9.446195	.058	.036
1074	7.1	7.094271	7.453652	6.4	6.746819	9.375465	.061	.036
1104	8.5	8.004973	8.28	6.4	5.911826	9.360411	.109	.043
1119	8.25	7.934380	8.15	5.5	6.263585	9.366750	.095	.043
1440	7.4	6.844487	7.24	7.9	7.806853	9.310594	.071	.032
1475	8.25	8.183471	8.29	7	7.595058	7.680057	.086	.077
1495	9.8	9.5	9.71	4.4	6.9	7.380808	.052	.07
SH 30 Slurry Seal								
2060	9.25		9.256710	7.5		5.261748		.059
2200	7.56		7.871681	6		6.493309		.09
2250	8.12		8.196817	5.75		6.061707		.077
2810	7.33		7.546359	5.75		6.772663		.091
2860	8.81		9.197975	6		5.644378		.084
2900	8		8.395410	6		5.375427		.034

SH 30 Chip Seal								
300	8.25		8.774581	7		6.967352		.0676417
350	9.75		10.36418	8.25		5.055375		.0463549
410	9.25		9.995161	7		7.181201		.0267325
445	9.31		9.832067	7.5		5.620923		.0535310
1050	9.25		9.939052	7		6.516026		.0292093
1090	8.75		9.438135	7		5.926560		.0545304
SH105 Thin Overlay								
85	1.75		1.621858	9		8.959467		.101
115	2.62		2.255117	9.5		9.040790		.104
150	2.87		2.777517	9.5		10.04532		.11
190	6.25		3.097718	9.5		9.954001		.115
735	2.62		2.471501	8		8.005818		.09
770	2.25		2.351285	8.5		8.614625		.143
790	2.25		2.004479	9		9.132111		.132
SH105 GPS Section								
6	2.3	2.709172	1.995276	8	9.617021	9.583601	.1160714	.1242385
101	1.62	2.498900	1.777788	9	8.738990	9.550485	.1272727	.1374088
166	1.9	2.503404	1.928807	7.5	6.917496	8.494461	.1160714	.0823121
202	1.5	2.323007	1.726657	8.8	8.545078	8.273742	.0952381	.0573575
257	2	2.774046	1.933821	7.3	9.162521	9.268148	.1132075	.1122768
432	1.87	2.052694	1.667116	8.5	8.184166	7.966383	.1028037	.0627333
447	1.9	2.027013	1.749412	8.4	7.852933	8.592125	.1089109	.0737055
452	1.9	2.028567	1.840158	8.4	7.918048	8.927853	.1226415	.0786962
457	1.8	2.082867	1.931180	9.6	7.117994	6.141677	.1067961	.0753676
462	1.9	1.902835	1.707455	9.6	7.155364	7.930633	.1470588	.0683230
1039	1.8	2.014217	1.574447	9.6	8.849915	7.783892	.0980392	.0779939
1059	1.6	1.911580	1.687741	8.8	9.396265	8.544052	.0660377	.0764073
1185	1.6	1.993459	1.784611	8.4	9.749399	8.794466	.1214953	.1117088
1200	1.75	1.998543	1.673891	8.5	9.223949	8.574282	.1274510	.0897598

SH105 Slurry Seal								
1080	1.68		1.611594	8.5		8.389293		.0961364
1105	1.87		1.683307	8.5		8.920265		.1559949
1725	1.75		1.806400	8.5		9.602817		.1303538
1780	2.37		2.146979	9.75		10.82780		.0770795
1900	1.62		1.777788	9		9.583027		.1435346
SH105 Chip Seal								
3000	1.75		1.703403	8.5		8.630256		.0914667
3020	1.94		1.797537	8.5		8.623922		.1040665
3060	2.25		2.127457	8.25		8.818159		.1065501
US190 GPS Site								
145	2.75		2.241500					
205	2.75		2.762463					
305	3.37		2.919084					
380	2.5		2.206058					
430	2.75		2.269550					
455	3.12		2.785053					
480	3.12		2.755205					
4055	3		2.118515					
1200	3.12		2.129554					
1305	3		2.439796					
1405	2.62		2.190848					